INSTITUTE OF AERONAUTICAL ENGINEERING

(Autonomous)

Dundigal, Hyderabad -500 043

AERONAUTICAL ENGINEERING

IV B. Tech I semester (JNTUH-R15)

Experimental Aerodynamics

Elective II

Prepared by

Shiva Prasad U,

Assistant Professor, AE

UNIT-1
AERODYNAMIC EXPERIMENTS

Wind Tunnels

- Objective
  - Accurately simulate the fluid flow about atmospheric vehicles
  - Measure -Forces, moments, pressure, shear stress, heat transfer, flowfield (velocity, pressure, vorticity, temperature)

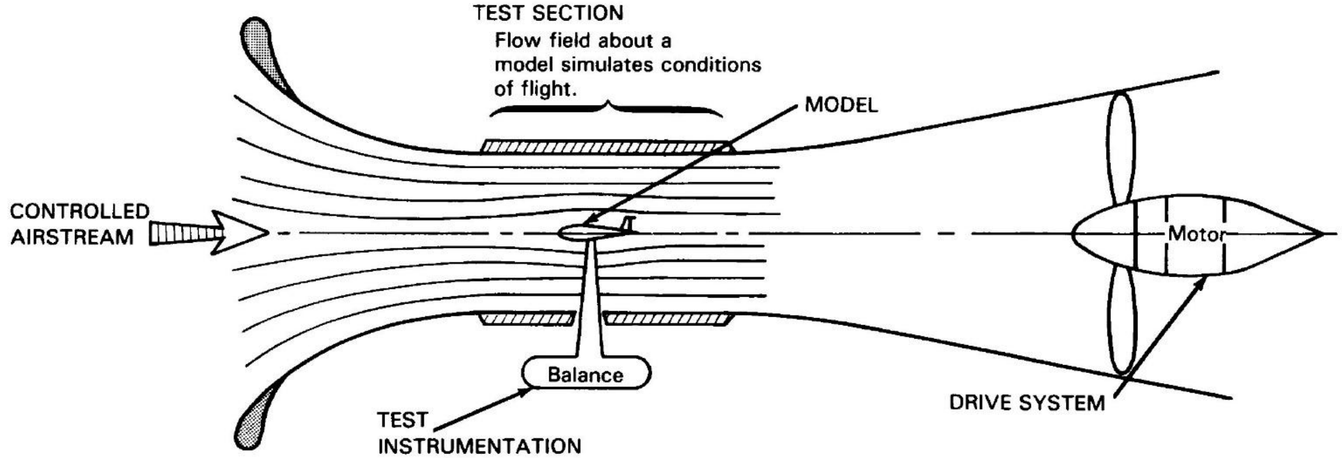

Low Speed Vehicles - M<.3

Gallilean Transformation

U_∞

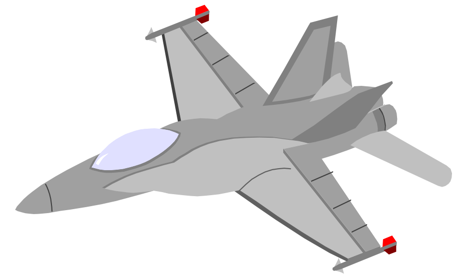

Flight in atmosphere
Scale =L

Wind Tunnel - Model Scale = ℓ

Stationary Walls

U_∞

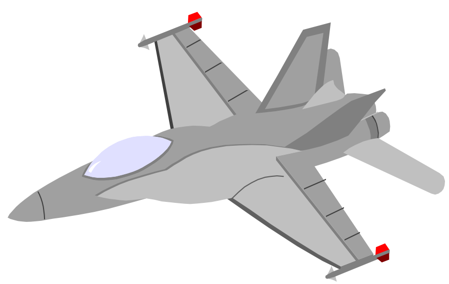

Issues

Flow Quality - Uniformity and
Turbulence Level

Wind Tunnel Wall Interference

Reynolds Number Simulation

$$\mathrm{Re} = \frac{\rho U_\infty L}{\mu} \neq \frac{\rho U_\infty \ell}{\mu}$$

• Must Match Reynolds Number and Mach Number

Transonic Regime .7<M<1.2

$$\mathrm{Re} = \frac{\rho U_{\infty} L}{\mu}$$

$$M = \frac{U_{\infty}}{c}$$

Must change fluid density and viscosity to match Re and M

Cryogenic Wind Tunnels are designed for this reason

History
Whirling Arm

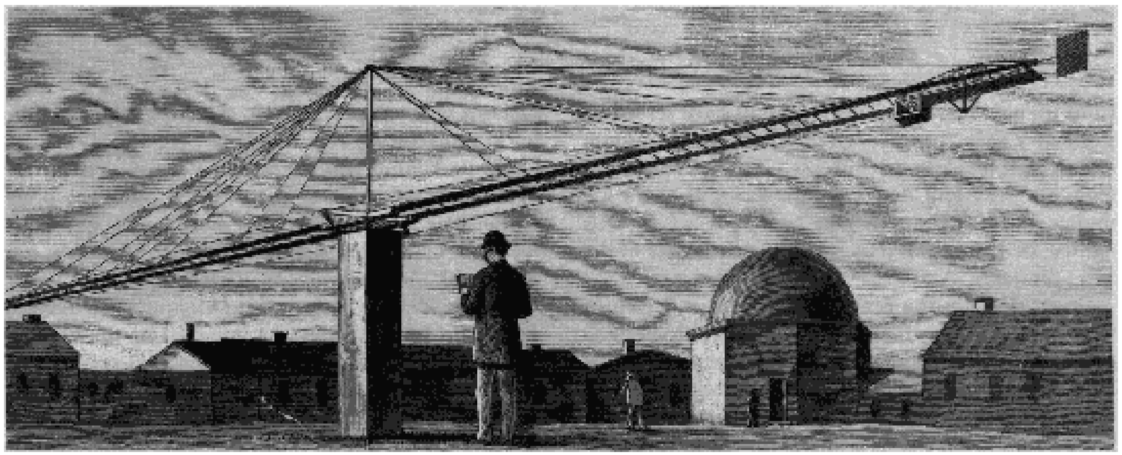

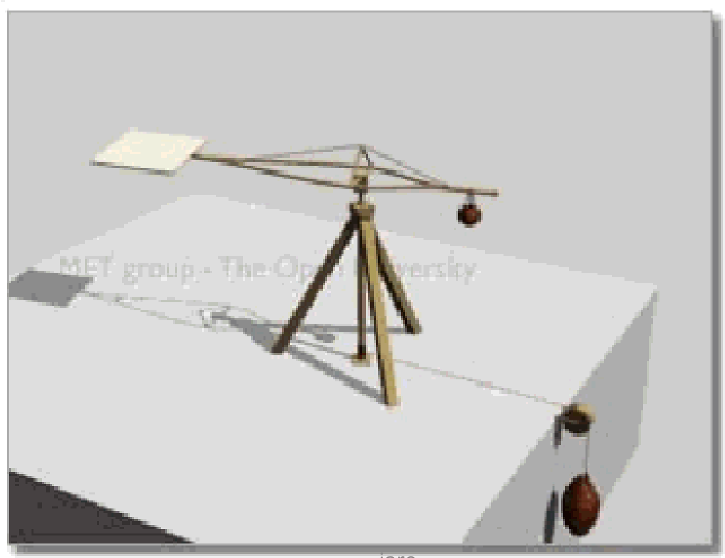

Eiffel Tunnel

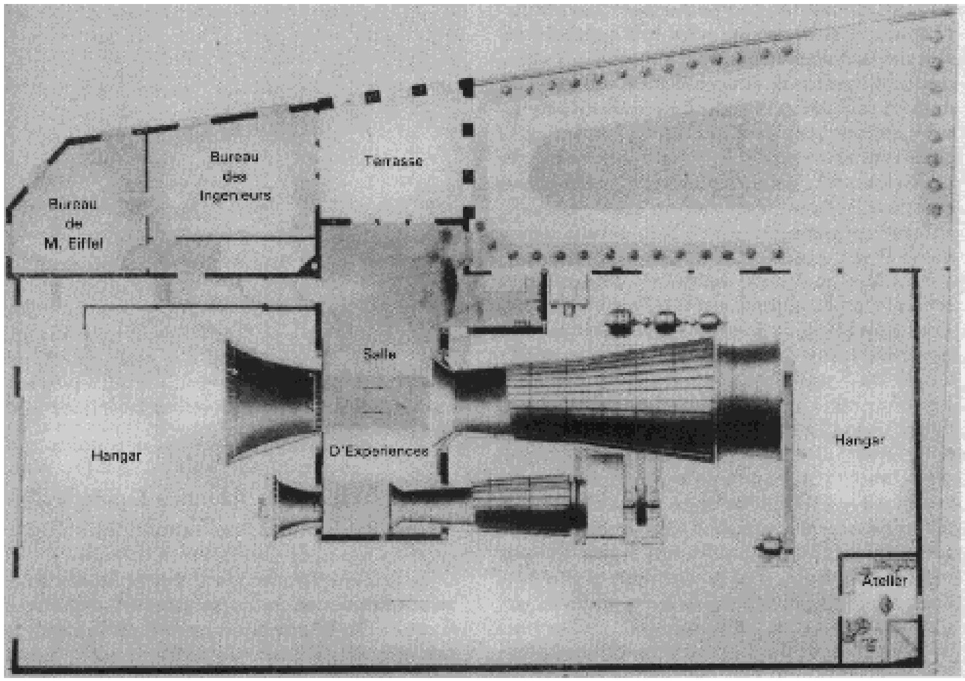

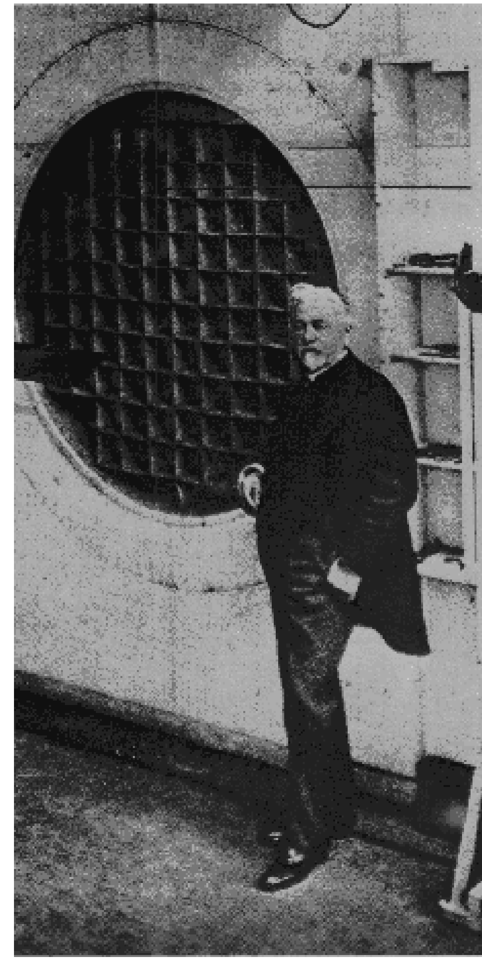

Wright Brothers

The Wright Brother's "Drift" Balance
(top view)

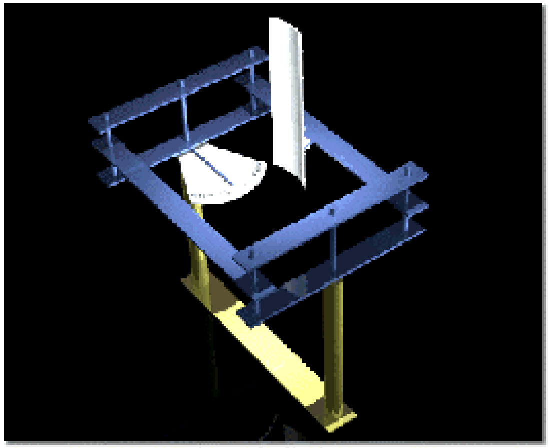

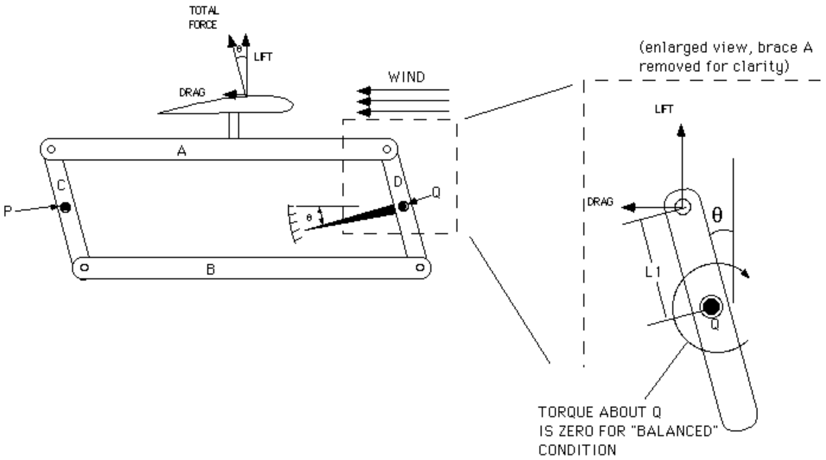

Wind Tunnel Test Trend

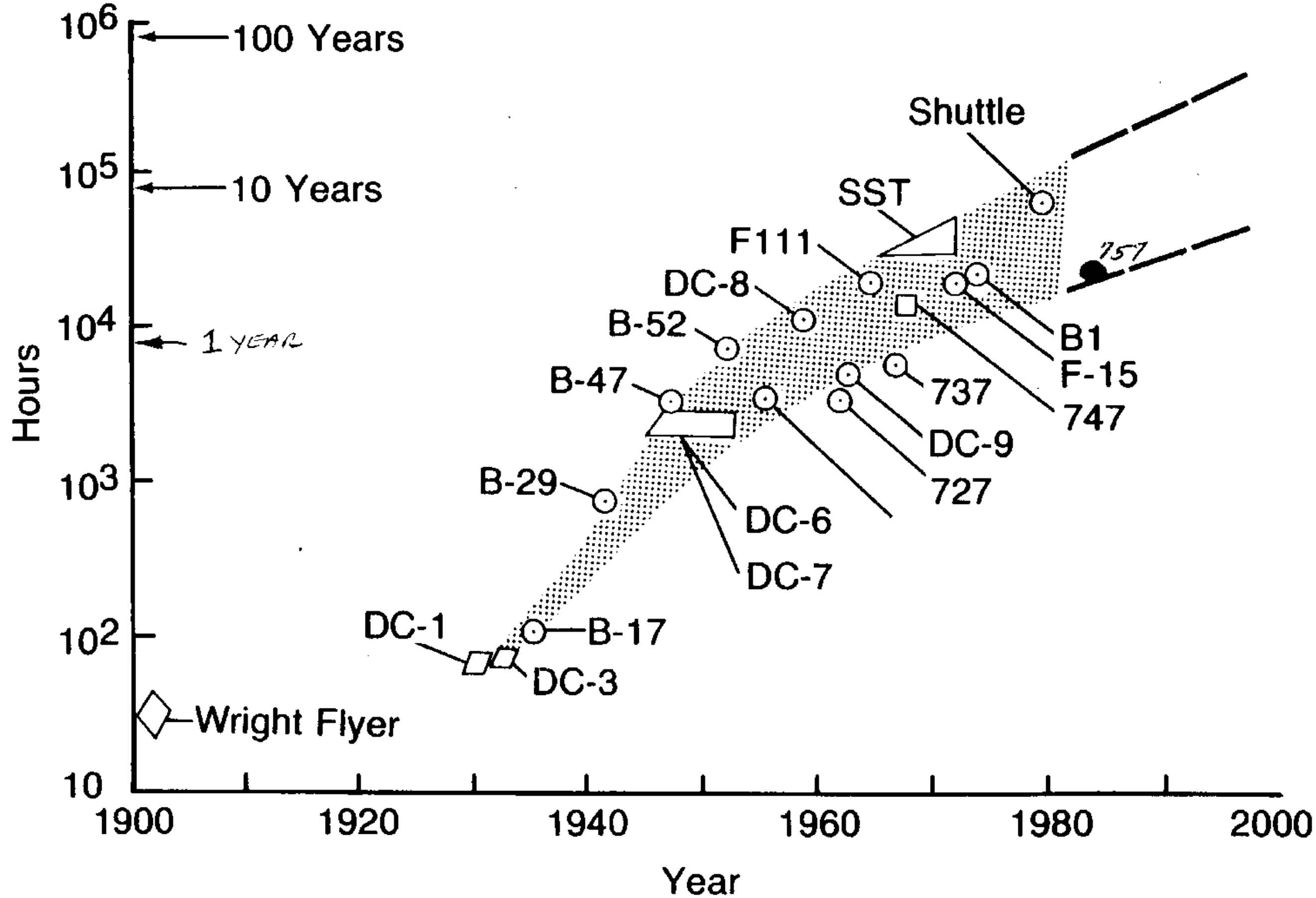

Wind Tunnel Layout

- Closed Return
- Open Return
- Double Return
- Annular Return

Closed Return
(open test section)

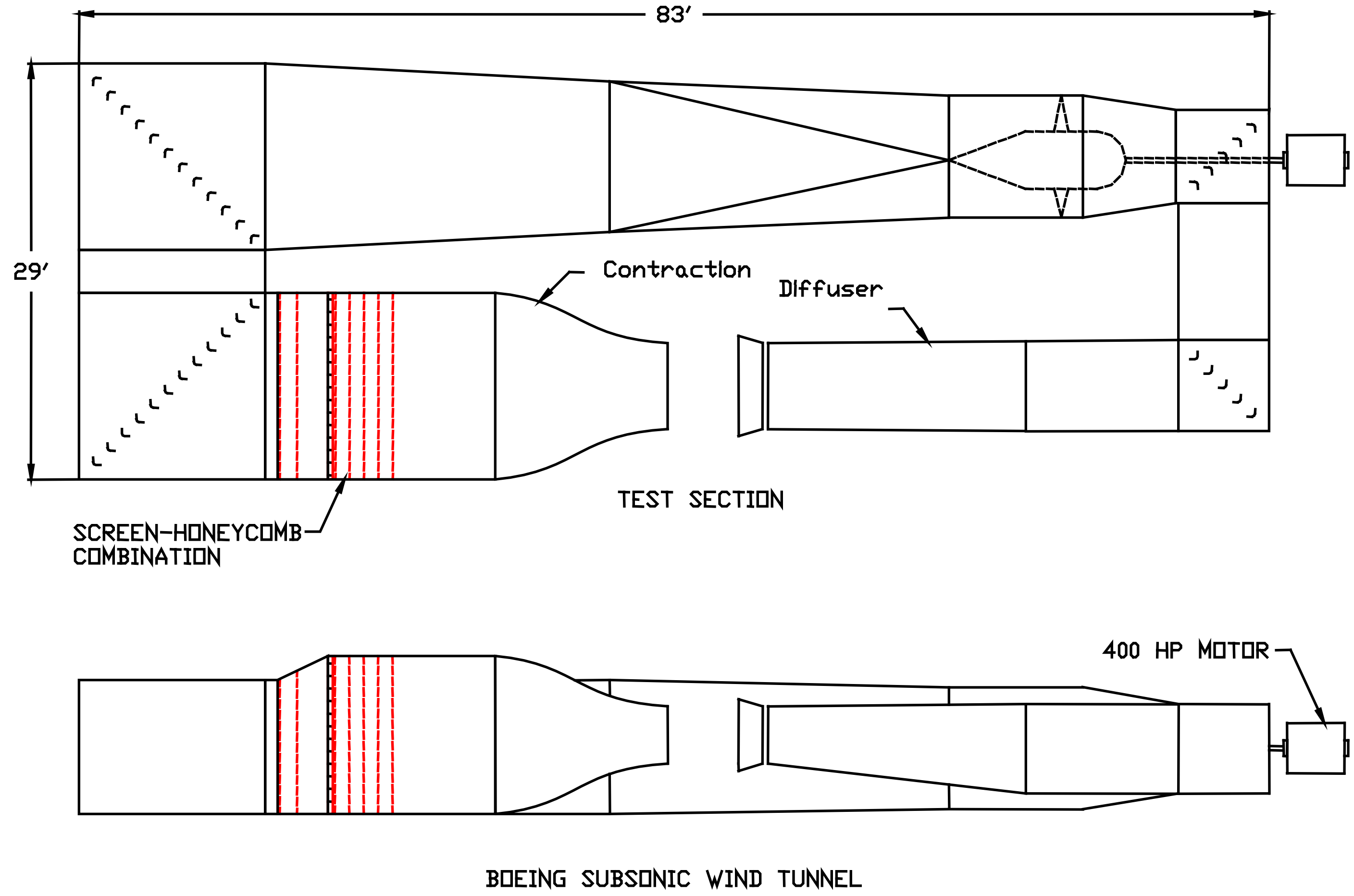

Open Return
Closed Test Section

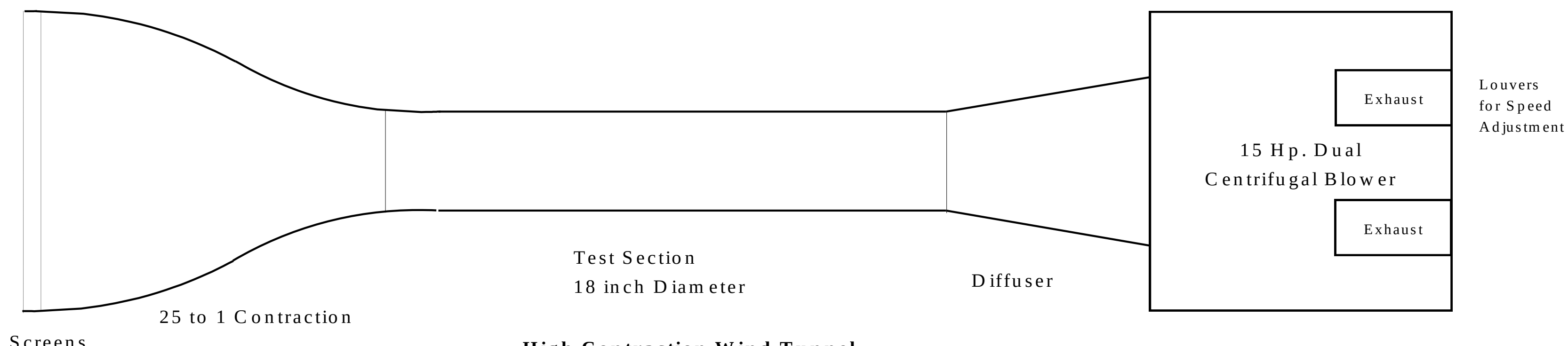

High Contraction Wind Tunnel
Top View

Double Return

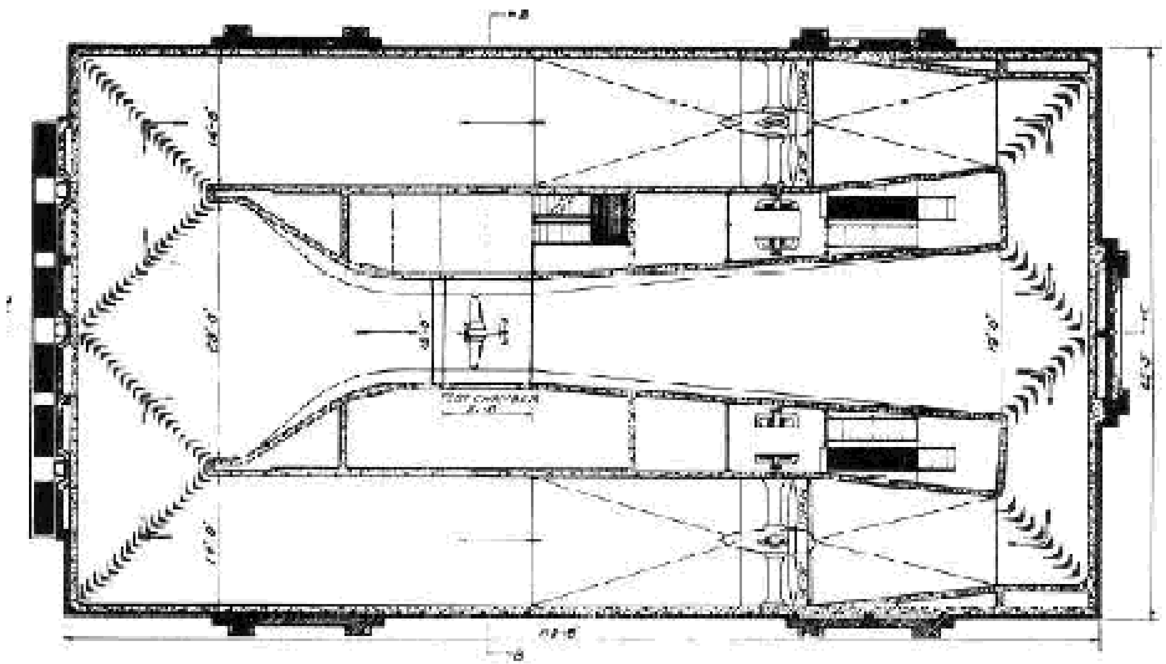

U N I V E R S I T Y OF W A S H I N G T O N
A E R O N A U T I C A L L A B O R A T O R Y
Kirsten Wind Tunnel

Annular Wind Tunnel

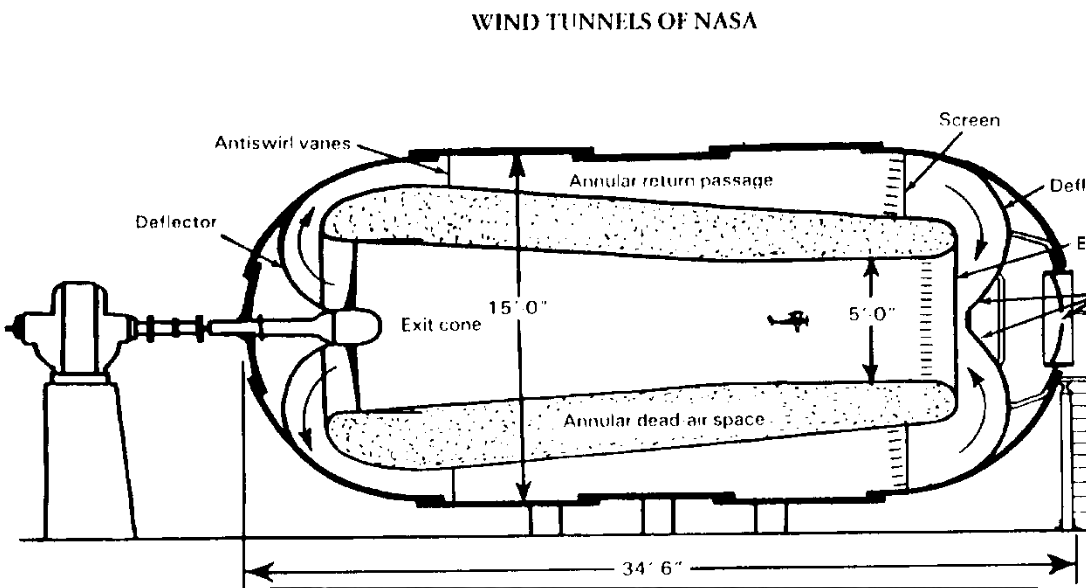

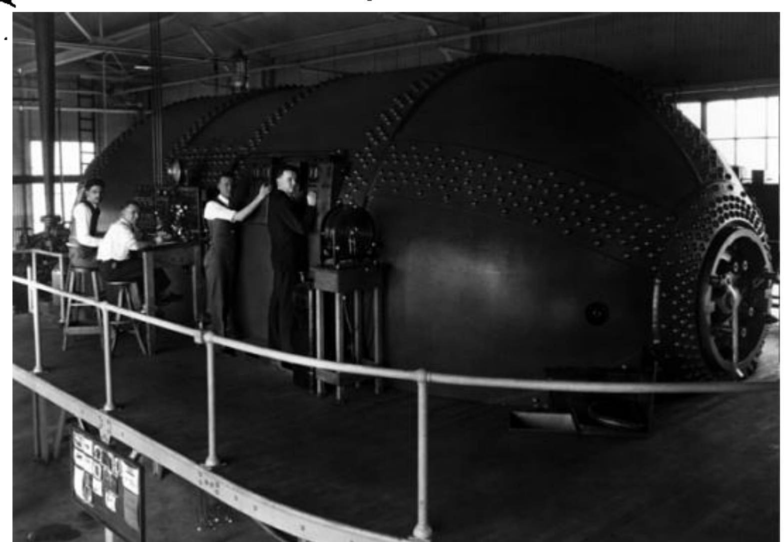

Variable Density Tunnel, Being Used by NASA Staff
NASA Langley Research Center 3/15/1929 Image # EL-1996-00143

Types of Wind Tunnels

- Subsonic
- Transonic
- Supersonic
- Hypersonic
- Cryogenic
- Specialty
  - Automobiles
  - Environmental- Icing, Buildings, etc.

Subsonic Wind Tunnels

40’ x 80’ and 80’ x 120’
NASA Ames

Fans for 40x80 and 80x120

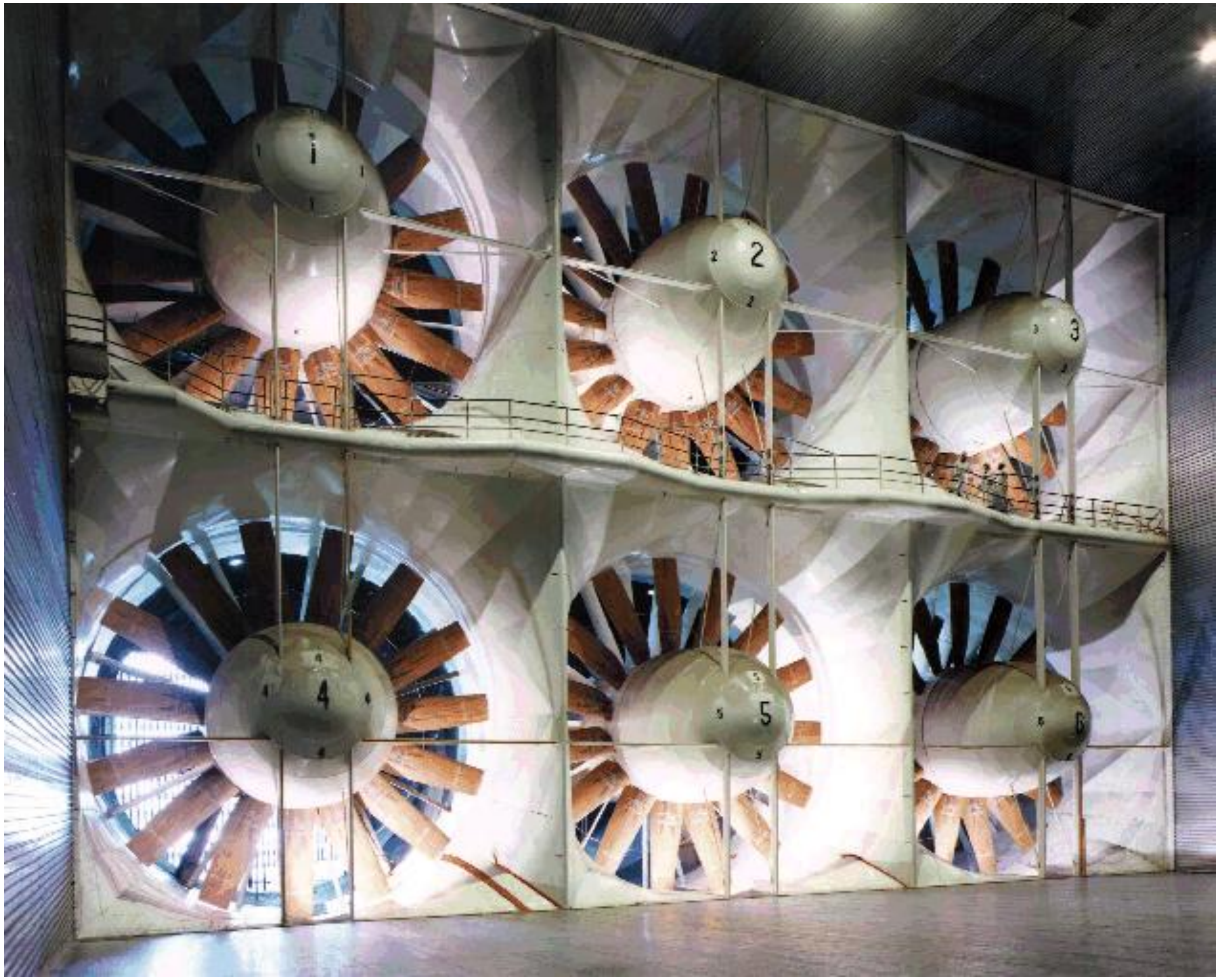

40’x80’

80’x120;

12 foot Pressure Tunnel

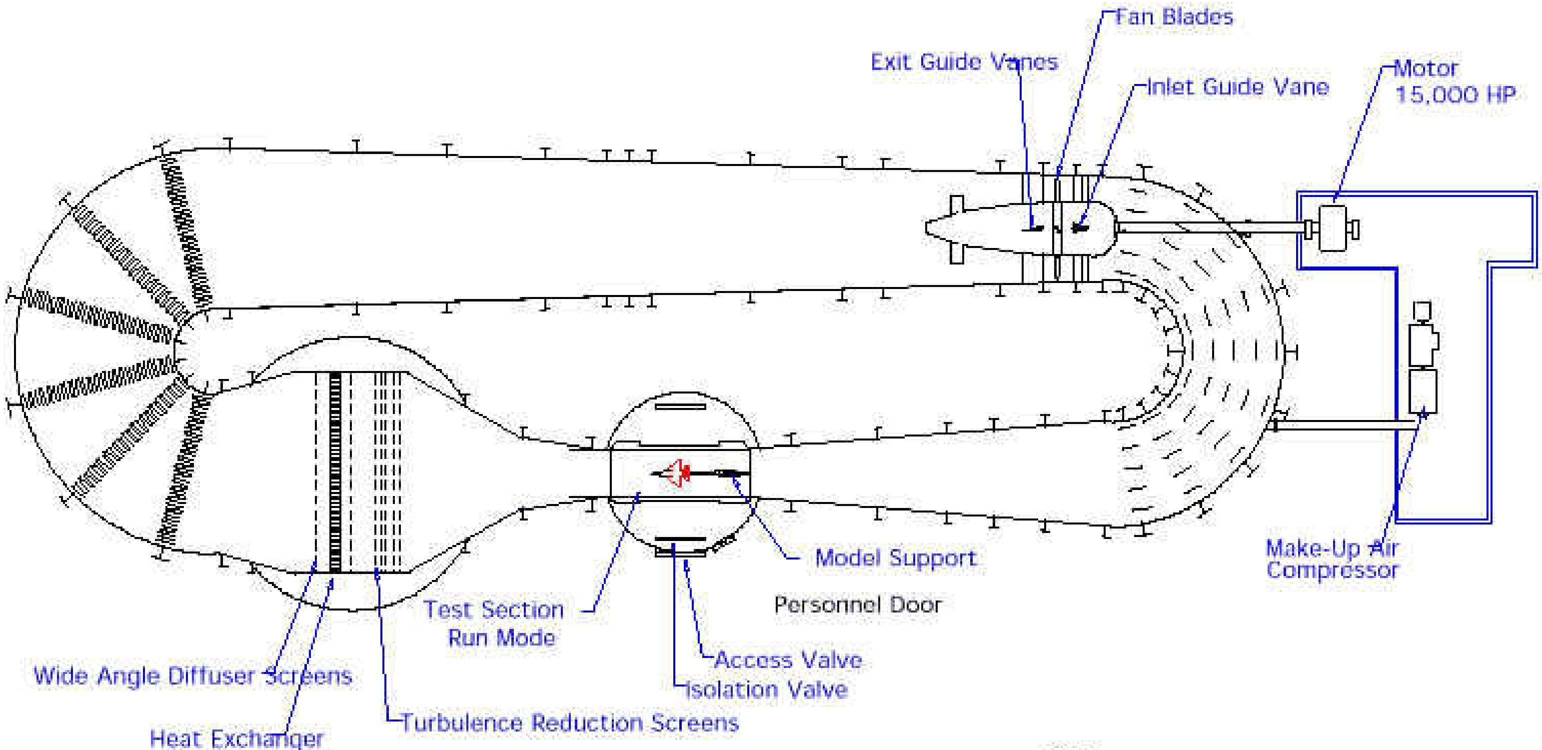

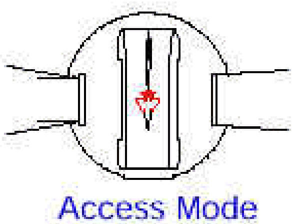

12ft Pressure Wind Tunnel
NASA Ames Research Center

12-Foot Pressure Wind Tunnel: Specifications

Primary Use:

The facility is used primarily for high Reynolds number testing, including the development of high-lift systems for commercial transports and military aircraft, high angle-of-attack testing of maneuvering aircraft, and high Reynolds number research.

Capability:

Mach Number: 0-0.52

Reynolds Number per foot: 0.1 - 12X106

Stagnation Pressure, PSIA: 2.0 - 90

Temperature Range: 540 ° - 610 ° R

Transonic
Wind Tunnels

Transonic Wind Tunnels

Wall interference is a severe problem for transonic wind tunnels.

Flow can “choke”

Shock wave across the tunnel test section

Two Solutions

Porous Walls

Movable Adaptive Walls

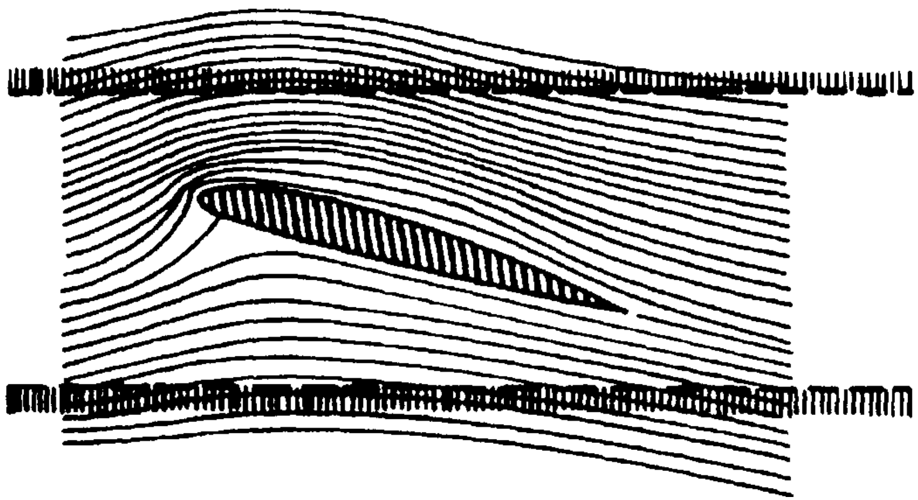

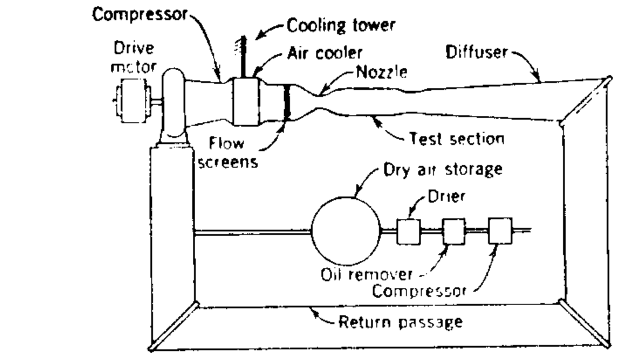

Fig. 1:1 Diagrammatic layout of closed-circuit, continuous flow, supersonic wind tunnel.

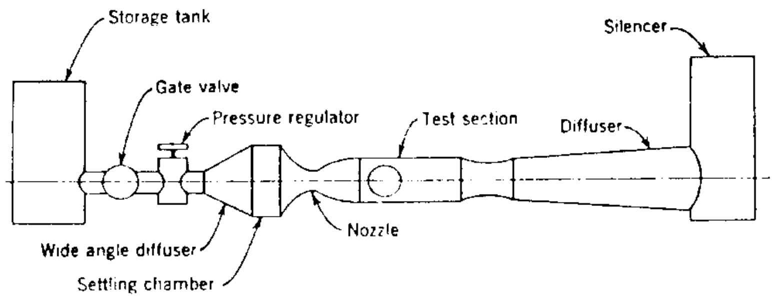

Fig. 1:2 Diagrammatic layout of intermittent blowdown tunnel.

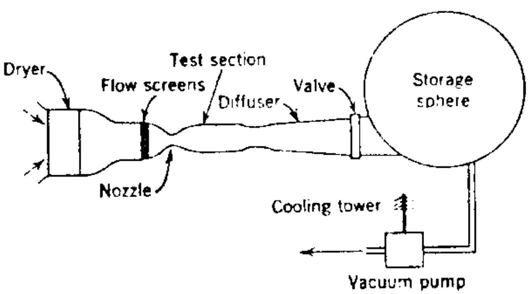

Fig. 1:3 Diagrammatic layout of intermittent indraft wind tunnel.

Purdue University
Aerospace Sciences Laboratory
M=2.5 Supersonic
Blowdown Wind Tunnel

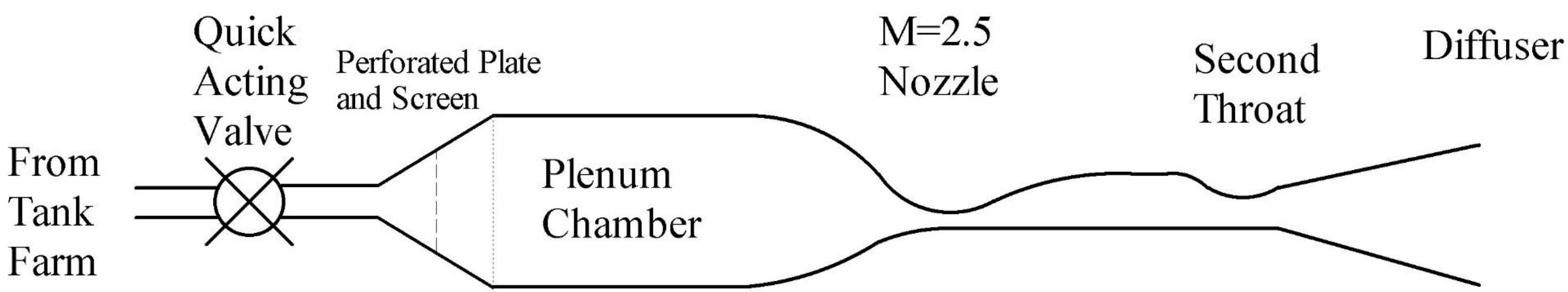

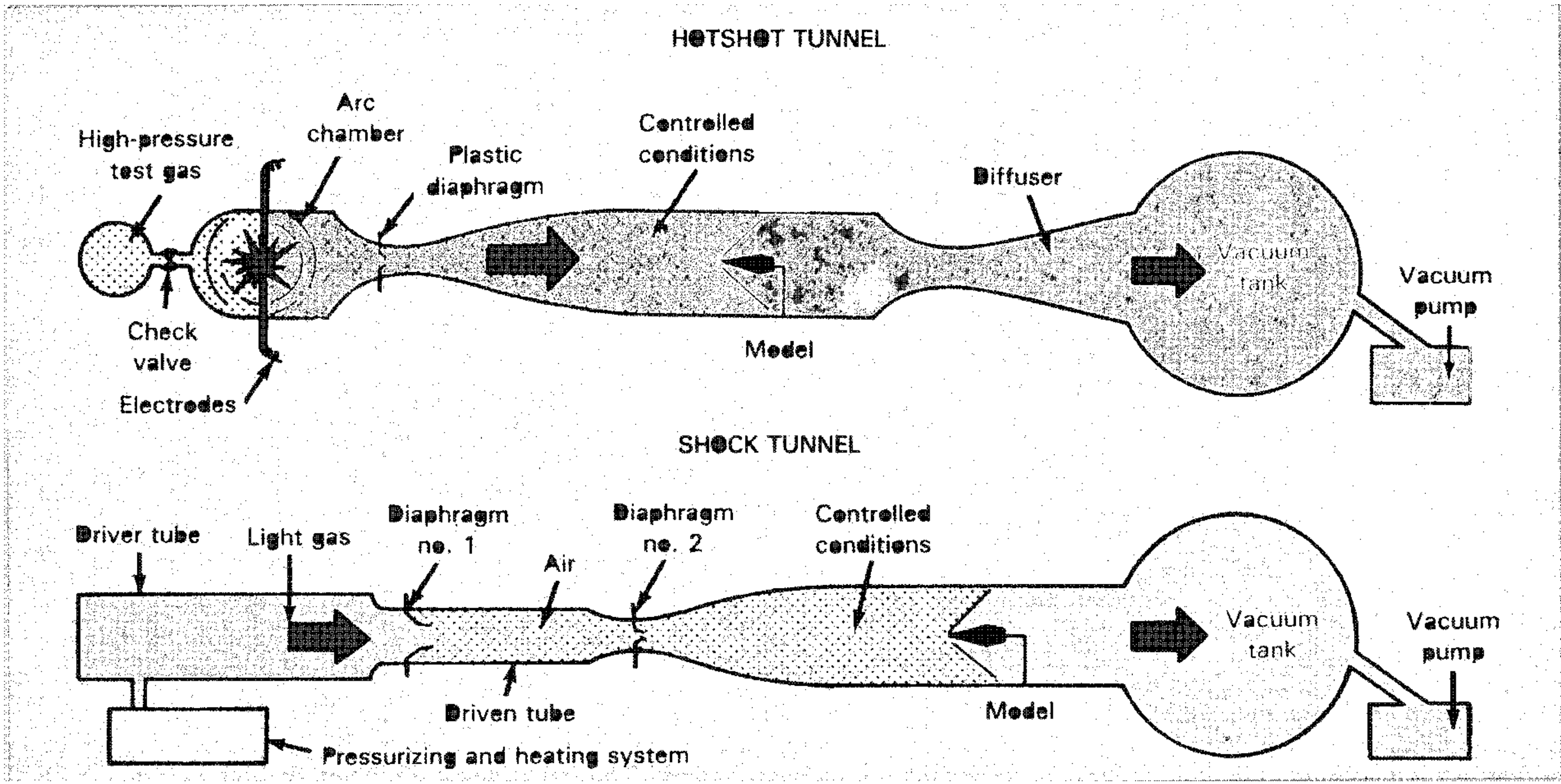

HOTSHOT TUNNEL
High-pressure test gas
Arc chamber
Plastic diaphragm
Controlled conditions
Diffuser
Vacuum tank
Vacuum pump
Check valve
Electrodes
Model
SHOCK TUNNEL
Driver tube
Light gas
Diaphragm no. 1
Air
Diaphragm no. 2
Controlled conditions
Vacuum tank
Vacuum pump
Driven tube
Model
Pressurizing and heating system

Principle Operation Detonation Driven Shock Tunnel

Set- up and wave plan:

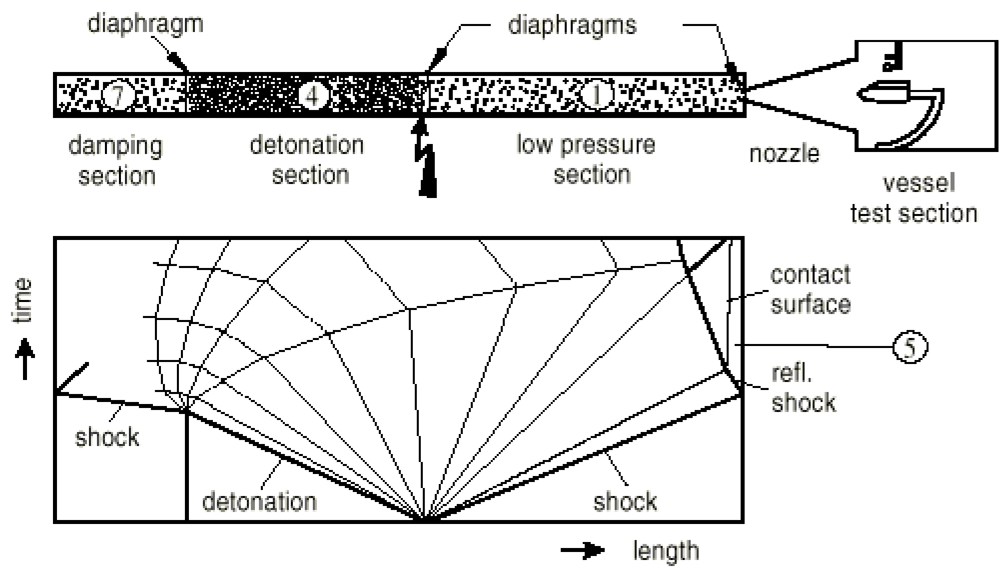

Initial conditions:

- low pressure section: test gas air, about 25 kPa for tailored cond.
- deton. section: oxyhydrogen- helium/ argon mixtures, max. 7 MPa
- damping section: expansion volume; low initial pressures

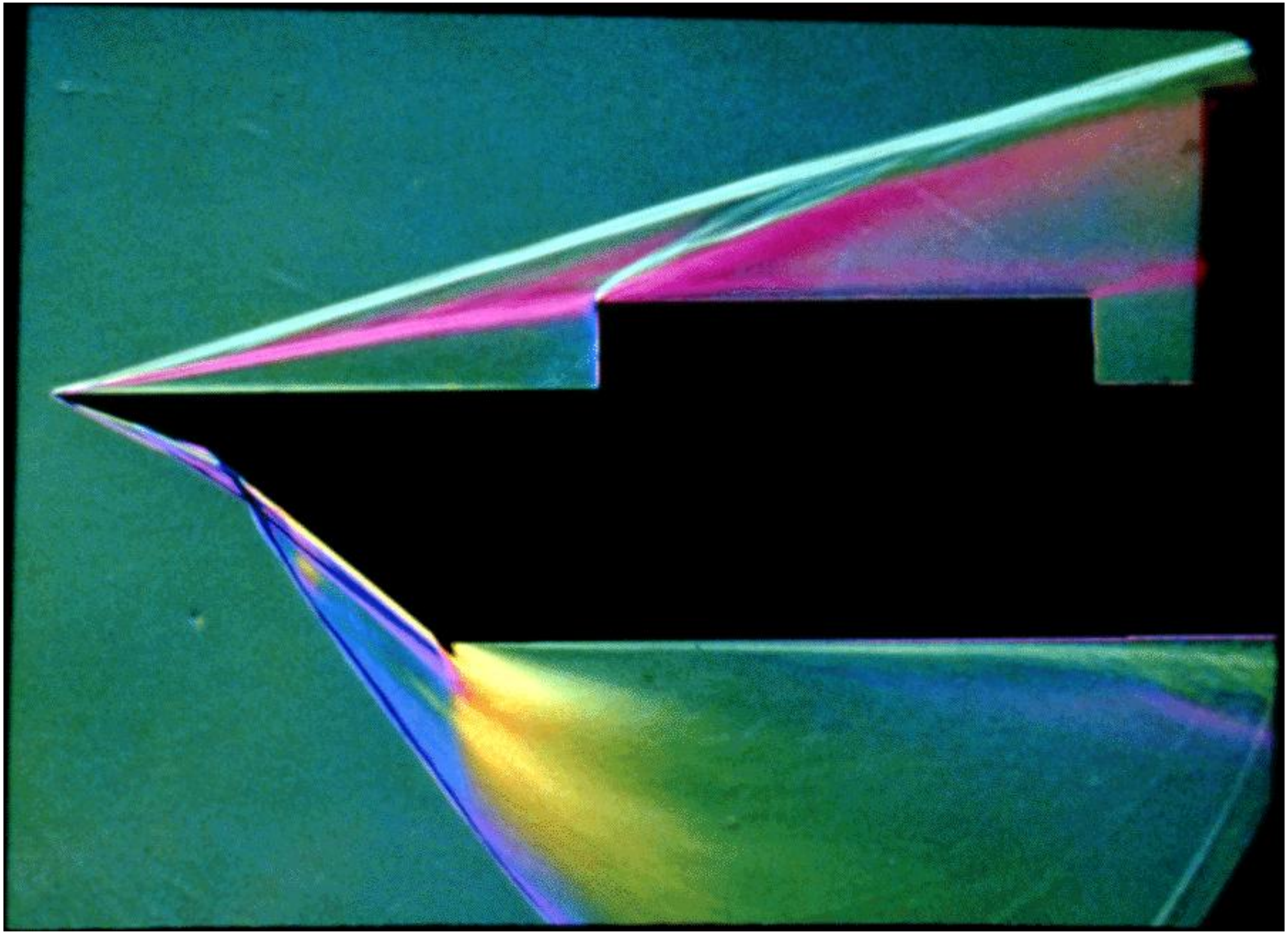

NASA
L-83-3,314

PRINCIPAL COMPONENTS OF THE NTF CIRCUIT

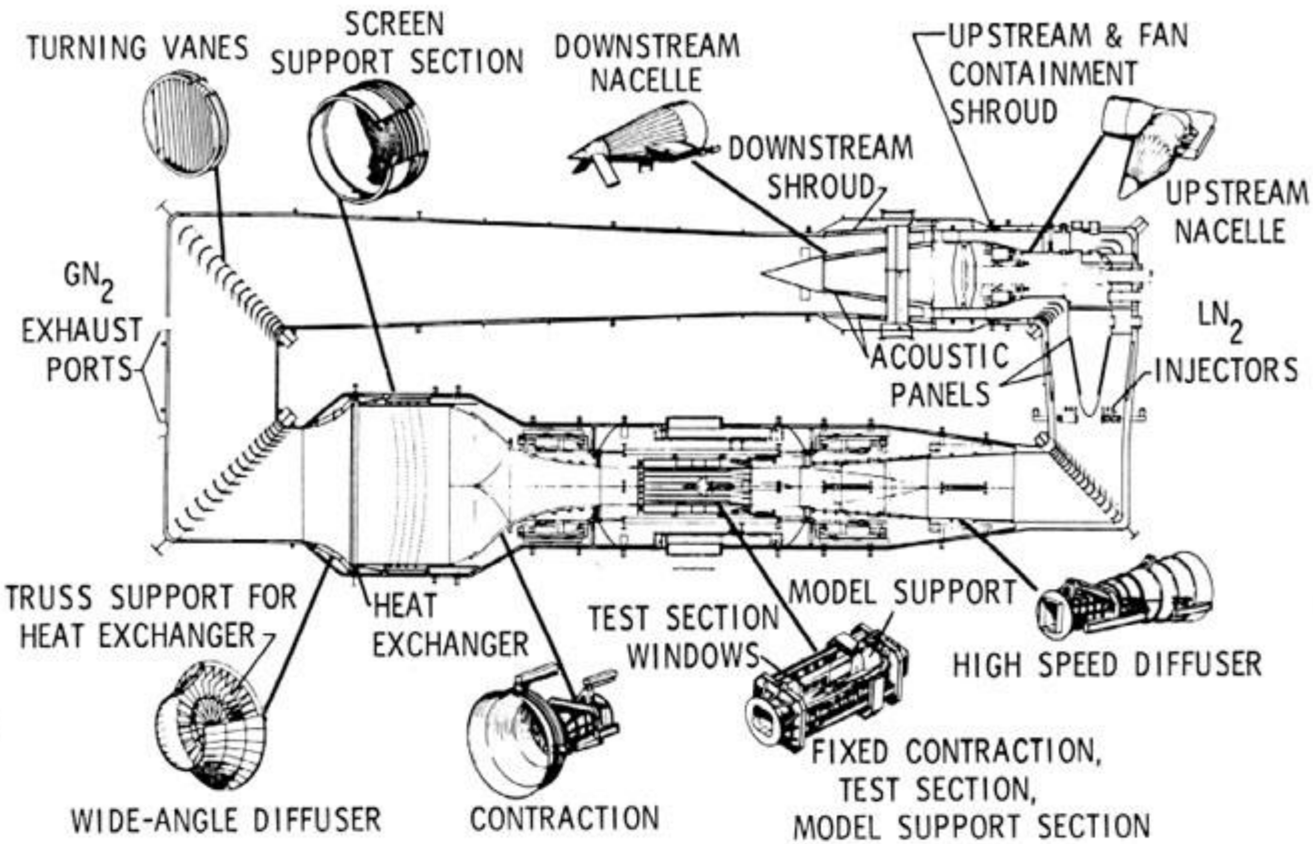

Cryogenic Wind Tunnels

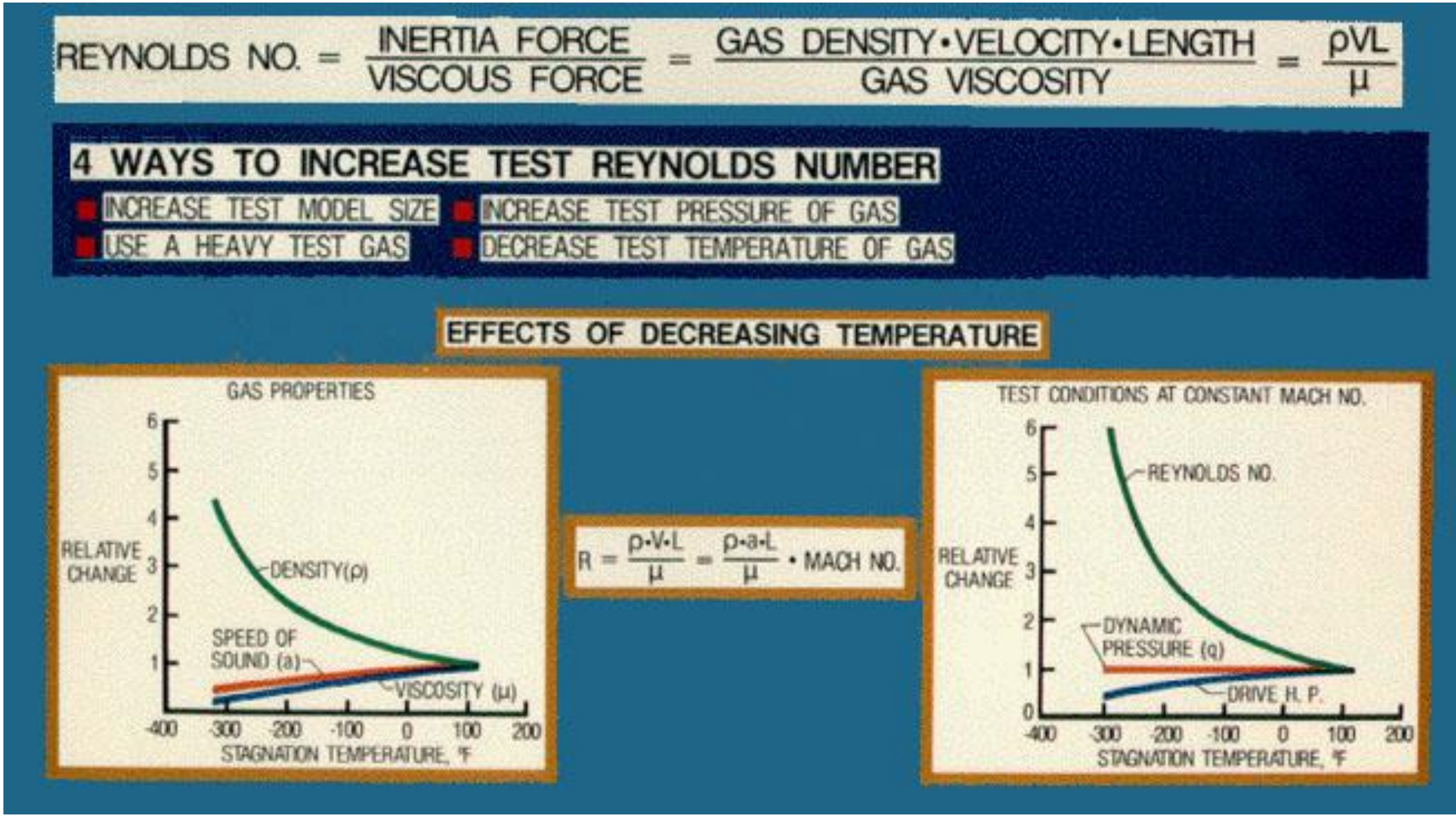
REYNOLDS NO. = INERTIA FORCE / VISCOUS FORCE = GAS DENSITY•VELOCITY•LENGTH / GAS VISCOSITY = ρVL / μ
4 WAYS TO INCREASE TEST REYNOLDS NUMBER
INCREASE TEST MODEL SIZE
INCREASE TEST PRESSURE OF GAS
USE A HEAVY TEST GAS
DECREASE TEST TEMPERATURE OF GAS
EFFECTS OF DECREASING TEMPERATURE
GAS PROPERTIES
RELATIVE CHANGE
DENSITY(ρ)
SPEED OF SOUND (a)
VISCOSITY (μ)
STAGNATION TEMPERATURE, °F
R = ρ•V•L / μ = ρ•a•L / μ • MACH NO.
TEST CONDITIONS AT CONSTANT MACH NO.
REYNOLDS NO.
DYNAMIC PRESSURE (q)
DRIVE H. P.
STAGNATION TEMPERATURE, °F

NATIONAL TRANSONIC FACILITY

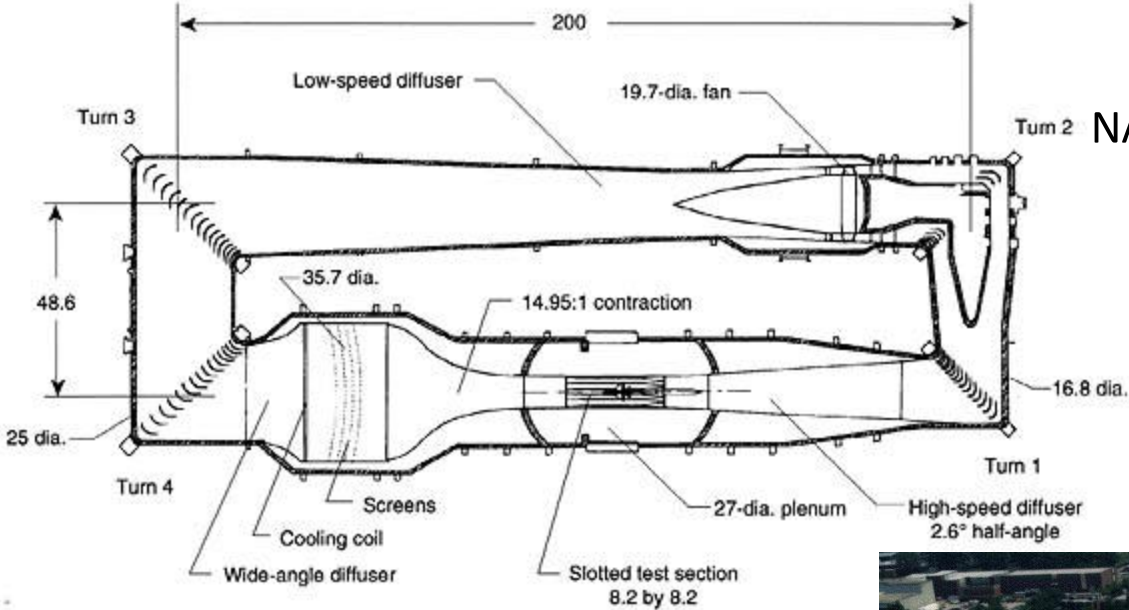

Figure 6. Plan view of NTF tunnel circuit. All linear dimensions are in feet.

The Cryogenic Ludwieg-Tube at Göttingen (KRG)

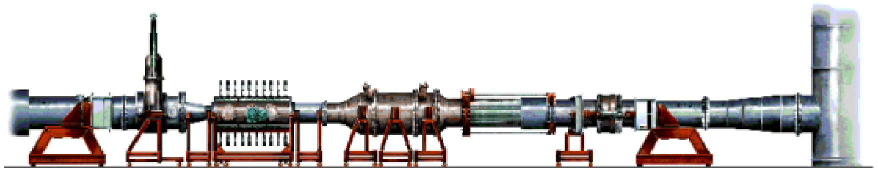

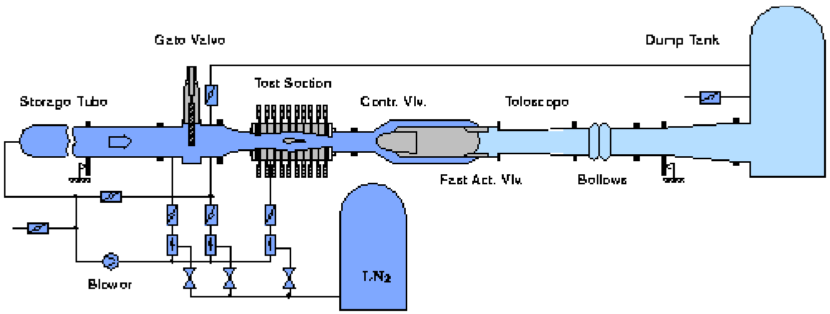

Tube	Diameter	0.8 m	Stag. press. (max.)	10 bar
	Length	130 m	Temperature range	100 to 300 K
	Load. press. (max.)	12.5 bar	Mach number range	0.25 to 0.95
Test Section	Cross section	0.4×0.35 m^2	Reynolds no. (max.)	$60 \cdot 10^6$
	Length	2.0 m	Run time	0.6 to 1.0 s
	Model chord (typ.)	0.15 m		

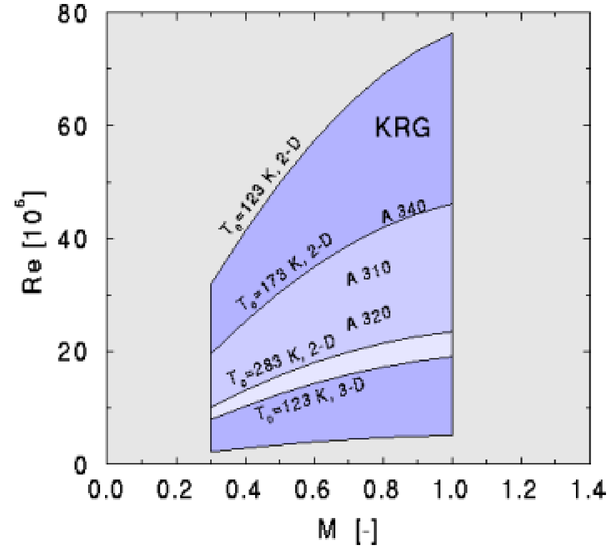

Adaptive wall test section

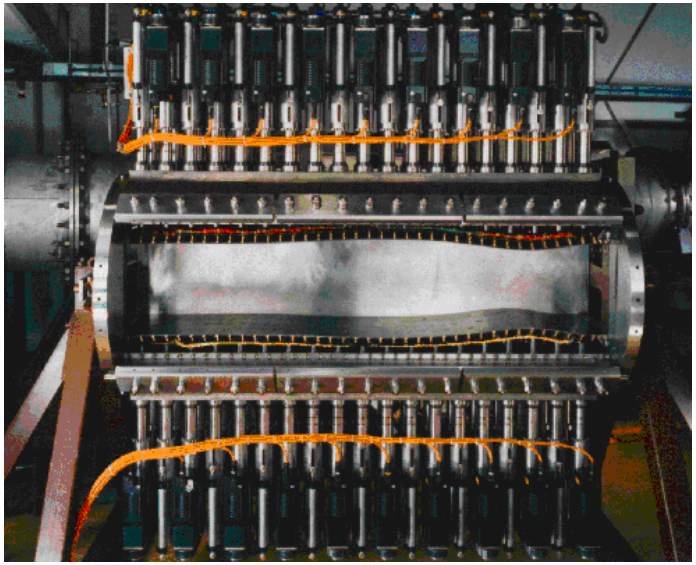

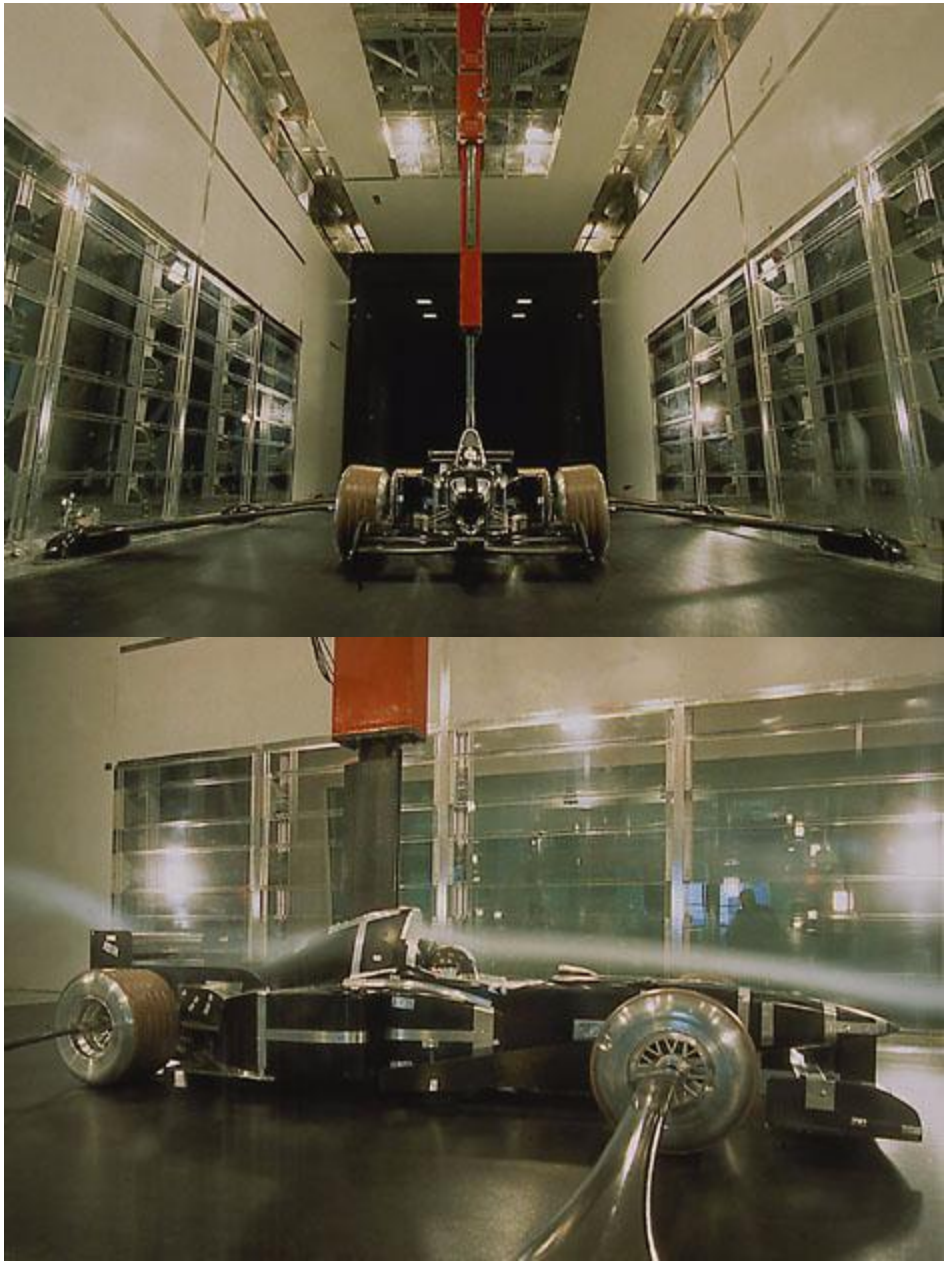

Automobile Wind Tunnels

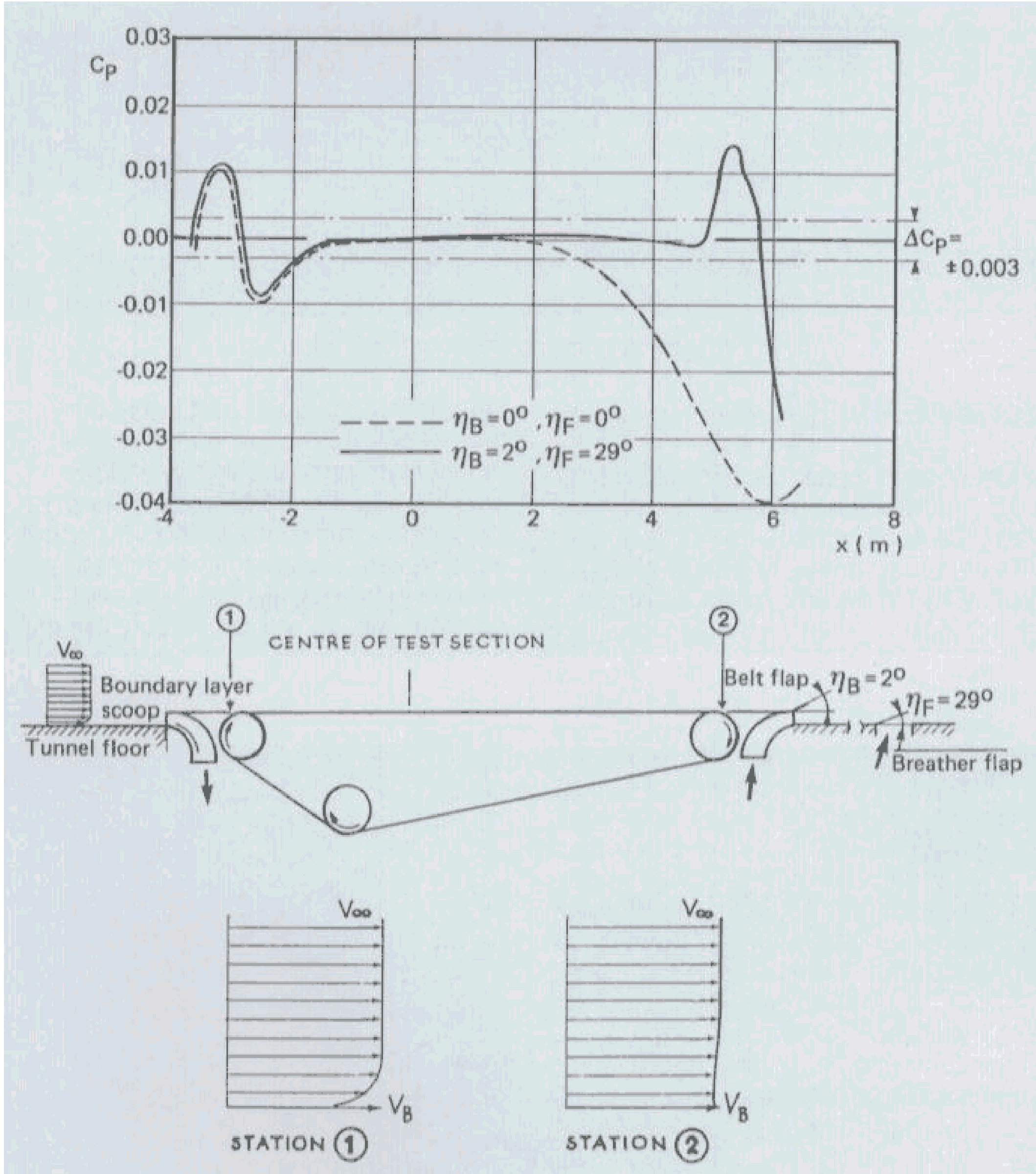

0.03
C_p
0.02
0.01
0.00
-0.01
-0.02
-0.03
-0.04
-4
-2
0
2
4
6
8
x (m)
$\Delta C_p = \pm 0.003$
$\eta_B = 0^o$, $\eta_F = 0^o$
$\eta_B = 2^o$, $\eta_F = 29^o$
1
2
CENTRE OF TEST SECTION
V_∞
Boundary layer scoop
Tunnel floor
Belt flap
$\eta_B = 2^o$
$\eta_F = 29^o$
Breather flap
V_∞
V_B
STATION 1
V_∞
V_B
STATION 2

Wind Tunnel Power Requirements

Energy Ratio

$$(E.R.)_t = \frac{\text{Jet Energy}}{\sum \text{Circuit Losses}} = \frac{1/2\,\rho_0 U_0^3 A_0}{\sum \text{Losses}} = \frac{q_0 U_0 A_0}{\eta P}$$

Subscript 0 refers to the test section

P is the motor power

η is the fan efficiency

Wind Tunnel Circuit Elements

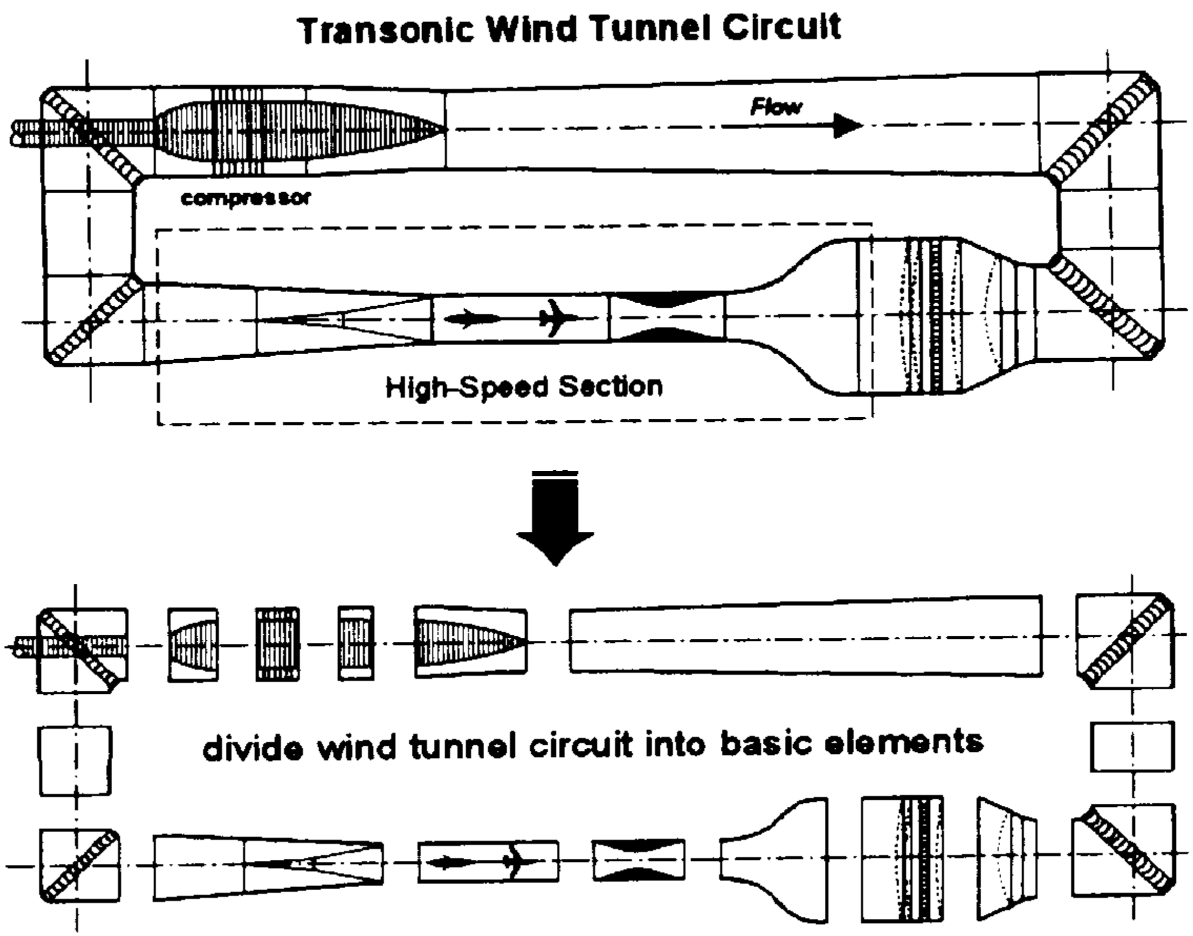

Losses

$$K = \frac{p_{t1} - p_{t2}}{q}$$ Local Pressure Loss Coefficient

$$K_0 = \frac{p_{t1} - p_{t2}}{q_0} = K \frac{q}{q_0}$$ Pressure Loss Referred to Test Section

$$\Delta E = K_0 1/2 \rho_0 U_0^3 A_0$$ Section Energy Loss

$$(E.R.)_t = \frac{\text{Jet Energy}}{\sum \text{Circuit Losses}} = \frac{1/2 \rho_0 U_0^3 A_0}{\sum \mathrm{K}_0 1/2 \rho_0 U_0^3 A_0} = \frac{1}{\sum K_0}$$

Closed Return Tunnel

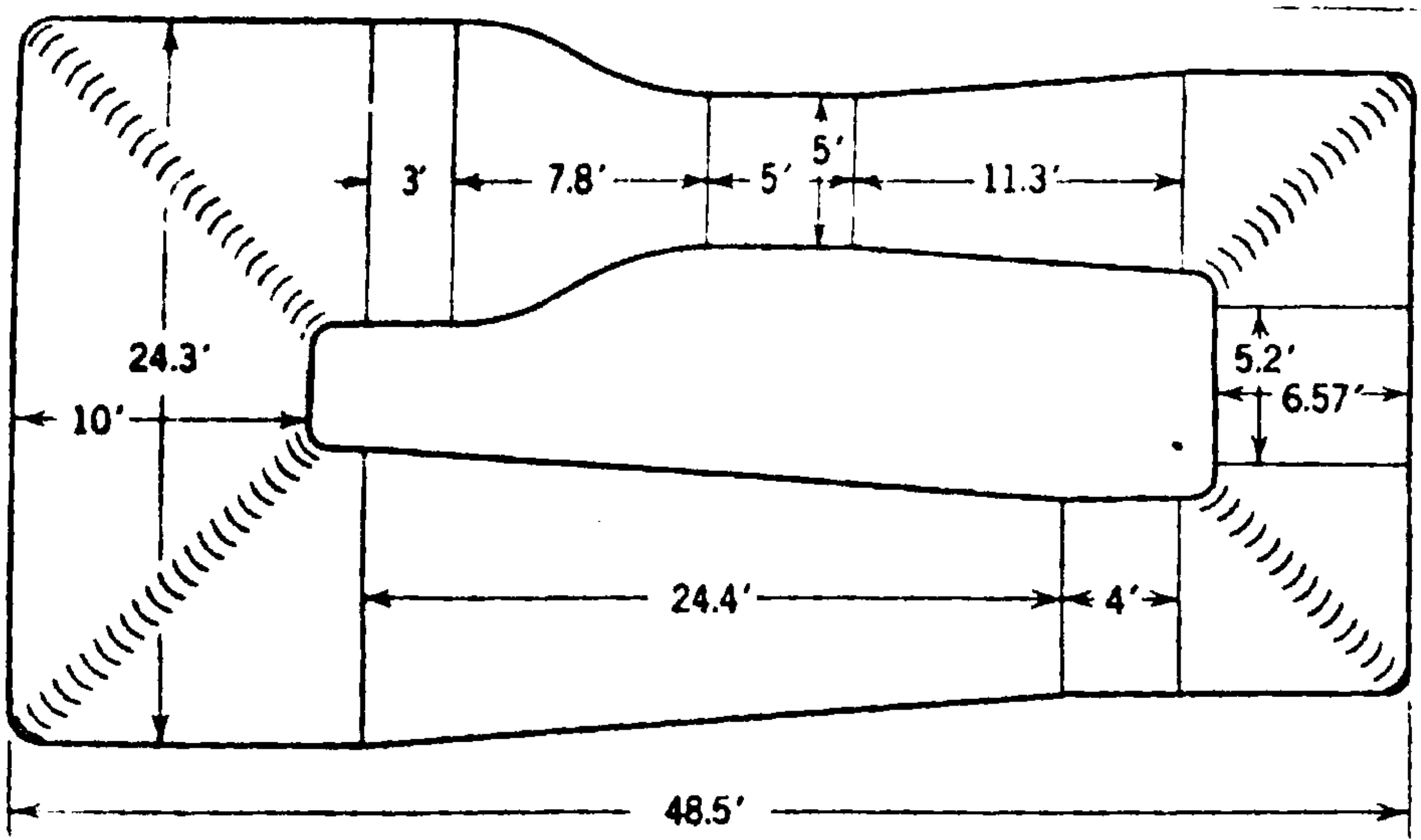

Example - Closed Return Tunnel

	Section	Ko	% Total Loss
1	Test Section	.0093	5.1
2	Diffuser	.0391	21.3
3	Corner #1	.0460	25.0
4	Straight Section	.0026	1.4
5	Corner #2	.0460	25.0
6	Straight Section	.0020	1.1
7	Diffuser	.0160	8.9
8	Corner #3	.0087	4.7
9	Corner #4	.0087	4.7
10	Straight Section	.0002	.1
11	Contraction	.0048	2.7
	Total	**.1834**	**100.0**

$$(E.R.)_t = \frac{1}{\sum K_0} = \frac{1}{.1834} = 5.45$$

Example - Open Return Tunnel

	Section	Ko	% Total Loss
1	Inlet Including Screens	.021	14.0
2	Contraction and Test Section	.013	8.6
3	Diffuser	.080	53.4
4	Discharge at Outlet	.036	24.0
	Total	**.150**	**100.0**

$$(E.R.)_t = \frac{1}{\sum K_0} = \frac{1}{.150} = 6.67$$

Turbulence Management System

Stilling Section - Low speed and uniform flow

Honeycomb - Reduces Large Swirl Component of Incoming Flow

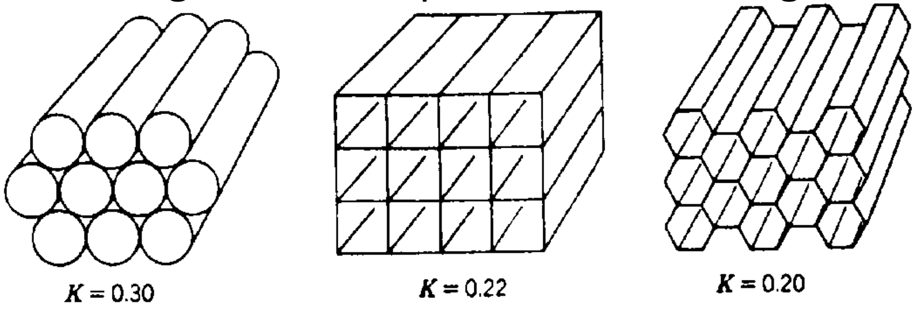

Fig. 2:16 Some honeycombs and their losses.

Screens - Reduce Turbulence [Reduces Eddy size for Faster Decay]
- Used to obtain a uniform test section profile
- Provide a flow resistance for more stable fan operation

Test Section

Test Section - Design criteria of Test Section Size and Speed Determine Rest of Tunnel Design

Test Section Reynolds Number
Larger JET - Lower Speed - Less Power - More Expensive

Section Shape - Round-Elliptical, Square, Rectangular-Octagonal with flats for windows-mounting platforms
Rectangular with filled corners
Not usable but requies power

For Aerodynamics Testing 7x10 Height/Width Ratio

Test Section Length - L = (1 to 2)w

Corners

Abrupt Corner without Vanes $\eta = 1.0$

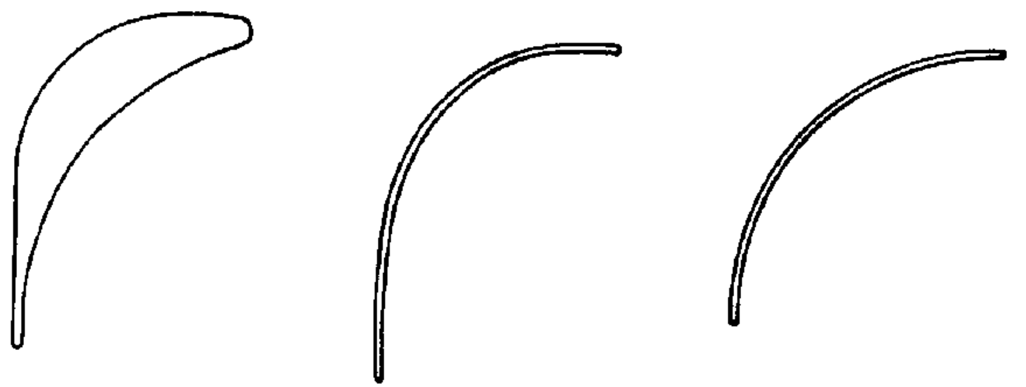

a $\eta = 0.11$ *b* $\eta = 0.138$ *c* $\eta = 0.20$

Low Speed Wind Tunnels-Detailed Design

Unit 2

Wind Tunnel Design

- Open-circuit or Straight through type.
  - Wright Brother’s tunnel
  - simple & very efficient
  - small open-circuit tunnels are usually inside a building
  - large tunnels must be open to outside are susceptible to dust ect.
  - Open-circuit tunnels are very noisy & surrounded by high wind current

Wind Tunnel Design

- Closed-Circuit or Return Type
  - Air is accelerated by the fan and flows through the tunnel
  - Turning vanes are installed to guide flow around the corner
  - The tunnel widens into a large settling chamber to decelerate the air; preventing a large build up of large boundary layer along the wall

Wind Tunnel Design

- Single-Return Type
  - all wind tunnels discussed thus far have been single-return
- Double Return Type
  - divides the flow downstream of the test section and runs through two circuits, each with a driving fan.
  - The flow then joins as it enters the settling chamber & proceeds through a single test section

Wind Tunnel Design

- Annular
  - An extension of the double-return concept
  - A return passage is located around the entire circumference of the wind tunnel outside the test section
  - This design was employed in the NACA variable density tunnel

Wind Tunnel Design

- Spin Tunnel
  - Special type of annular tunnel employed at Langley Research Center for spin research.
  - Is mounted vertically with the fan drawing air upward
  - Models are introduced into free-flight conditions then vertical flow adjusted

Types of Wind Tunnel Tests

- Original testing in wind tunnels was to a provide a means to determine lift & drag on airfoil shapes.
- Force Test
  - Force measurement requires a force to be exerted (lift & drag forces so termed force test)
  - The balance can measure only two forces: lift & drag

Six-Component Balance

- A more complete balance that can measure all six measures & moments about all three axes of the airplane
- Six component wind tunnel balance
  - this balance measures forces by use of strain gauges

Types of Wind Tunnel Tests

- Pressure Tests
  - Insert tiny tubes into the model surface or airstream and connect them to a pressure measuring device
  - Liquid Manometer-pressure measuring device
    - Tiny hole (pressure taps) drilled into the top of the surface, series of tubes, water added & measured

Types of Wind Tunnel Tests

- Lowered pressure over the wing surface reduced the pressure in the manometer tubes and draws the water level up to a high level
- The lower the pressure, the higher the water level goes
- Measuring the difference in water level will show the relative pressure difference

Types of Wind Tunnel Tests

- Flow Patterns
  - Allow the streamlines of air flow to look at the body's aerodynamic properties
  - Tufting allows for the flow pattern visualization
  - Tufting –the attachment of small tufts of yarn to the surface
  - The tufts will show if flow is attached or separated to form a wake.

Types of Wind Tunnel Tests

- Flow pattern
  - visualized by the use of smoke at the Embry-Riddle smoke tunnel
  - Smoke is generated by burning oil; then injected into into the airstream
  - Oil flow techniques can also be used to study flow patterns

High Speed Wind Tunnels

- Supersonic tunnels-1st developed in Germany, Busemann who also developed the swept-wing concept
- Early supersonic tunnels were the blow down type at Mach 1
- One of the most difficult conditions to create the flow at exactly Mach 1

Wind Tunnel Testing Problems

- Wall Effect
  - Walls are artificial boundaries that airplanes do not have
  - Upwash/downwash from walls, floors, ceiling
- Scale Effect
  - Small models have small forces making measurements inaccurate
  - Differences in Reynolds number between model and the full-scale model

Flight Testing

- Shakedown Tests
  - Basic flight qualities are determined
- Airplane’s Performance
  - An exact determination of top speed, cruise speed, range, rate of climb, takeoff & landing distance
- Stability & Controllability
  - Exact degree of stability, handling qualities

Flight Testing

- Performance
  - Special instruments take measurements in test flights
- Pressure Measurements
  - Attaching pressure measuring devices to taps on the aircraft surface
- Flow visualization
  - Tufts similar to wind tunnel testing
  - Reveal poor aerodynamic characteristics

Unit 3
High Speed Tunnels and Low speed Balances

- **DH bearing pedestals** are designed for the following applications: Low speed balancing
- Checking of rotor balance at high speeds (operational speed)
- Dynamic straightening of flexible rotors
- Testing of material strength by operating rotors at over speed
- Rotor investigation in operational bearings.
- All these tasks can be performed in a single rotor set up. The most important features of these high-speed balancing systems are shown on the next page.

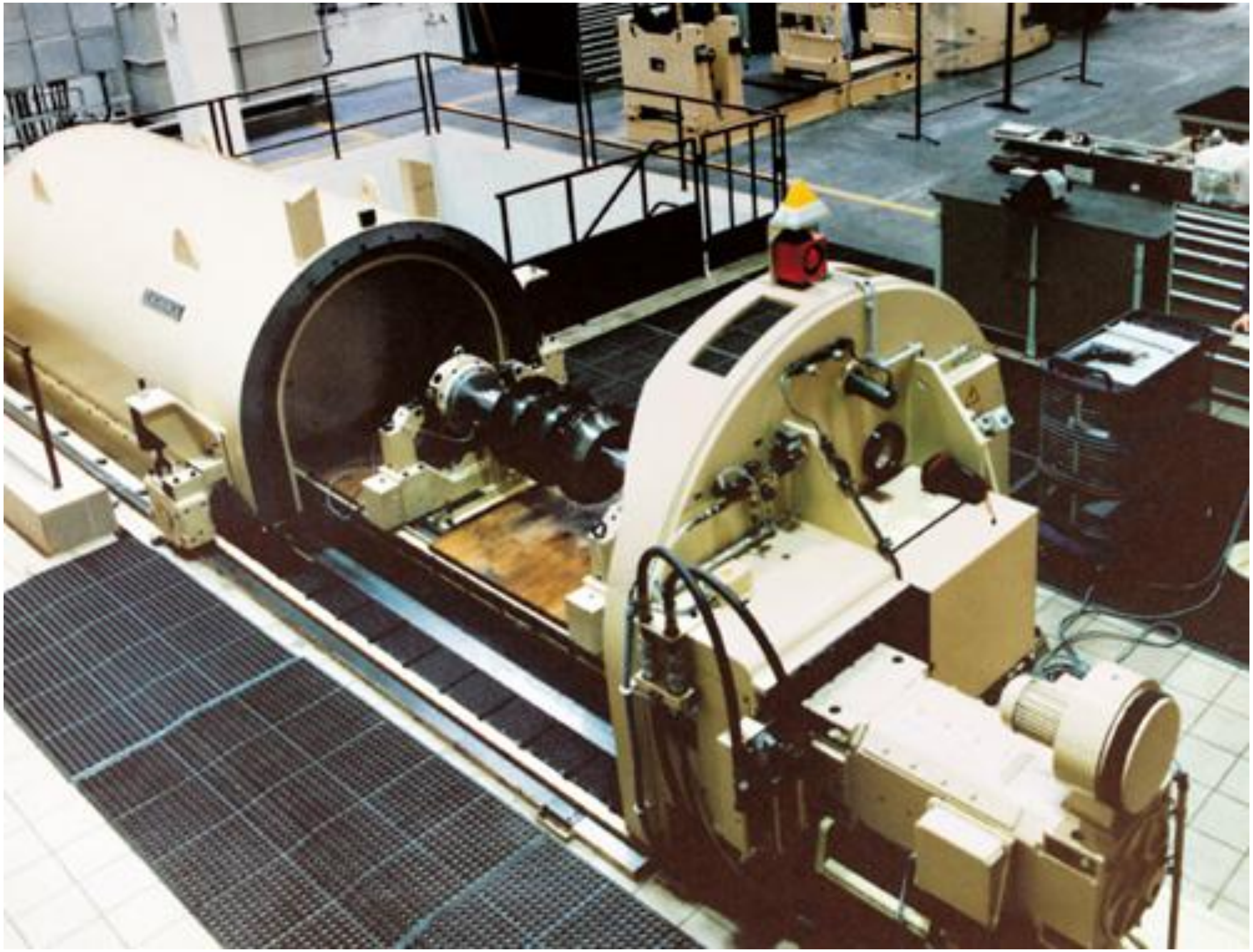

- **Rigid bearing supports – Additional stiffness**

  Rigid bearing supports provide for greater stability, particularly at high speeds. A supplementary, remote controlled change-over facility enables the stiffness of the bearing pedestals to be varied, thus enabling rotor resonance frequencies to be passed through safely, and minimizing the risk of damaging the rotor or the balancing facility.

  Balancing and overspeed testing under vacuum
  Due to the high windage effect of bladed rotors at high speeds and the associated power and temperature problems, balancing and overspeed testing takes place under vacuum conditions with a residual pressure of approx. 0.5 - 2 mbar.

- **Explosion proof enclosure**

To protect the surroundings from the dangers resulting from a total or partial explosion of the rotor, a variety of different solutions can be recommended:

Longstanding experience has shown that a walk-in tunnel design is most suitable, especially for medium or large facilities For rotors weighing up to 8 t, with outer diameters up to 1.7 m, an axially sliding vacuum chamber with integrated burst protection can be used. The movable part of the chamber is equipped with several steel liners, which act as burst protection. If the specimen bursts, the burst energy is absorbed by deformation elements in the foundation. A compact design enables the facility to be installed on the shop floor.

- **Drive system**

For high-speed balancing, overspeed testing and dynamic straightening of flexible rotors, either a three-phase servo motor with frequency converter or an infinitely variable DC motor with thyristor control can be used . Depending on the required speed range, a suitable transmission gear has to be installed. A so-called intermediate shaft constitutes the connection between the gear and the over-speed testing chamber. Rotors are coupled to this intermediate shaft by means of precision drive shafts.

Automatic Balance Calibration System

- Complete calibration (including installation, preparation of load schedule, load phase, full data reduction & balance removal) with 1000 loading points completed in about 3.5 hours.
- >0.1% accuracy preserved in any force combinations.
- Four safety loops ensure balance and machine integrity throughout the calibration.
- Calibration loads are applied exactly as in the wind tunnel for maximum calibration accuracy and reliability.
- Back-calculated errors can be displayed graphically in real time for quick evaluation.
- Inherent reliability and long term accuracy.
- Calibration of single piece and two shell balances up to 2.5" diameter.

Balances

- The balances are defined using aircraft design software (UGNX) and finite element software. The design is optimized according to customer-specified parameters (dimensions, loading and interfaces) and with respect to measurement requirements for sensitivity and stiffness.
- **Balance Types:**
- 6 component sting balance
- 1-5 component hinge moments balance
- 4-6 component fin balance
- Wing tip balance
- Half-model balance

Balances




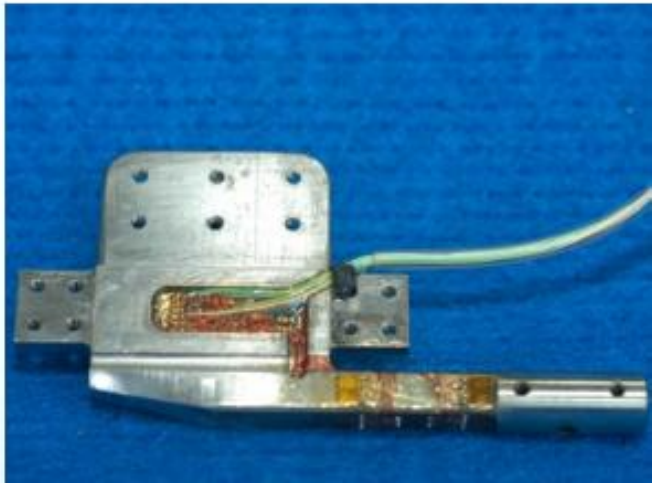

General arrangement of A.R. g jet-flap model

- To illustrate various aspects of the test arrangement devised, it is convenient to discuss the specific model details, the air-bearing rig assembly, and the recording system, in turn.

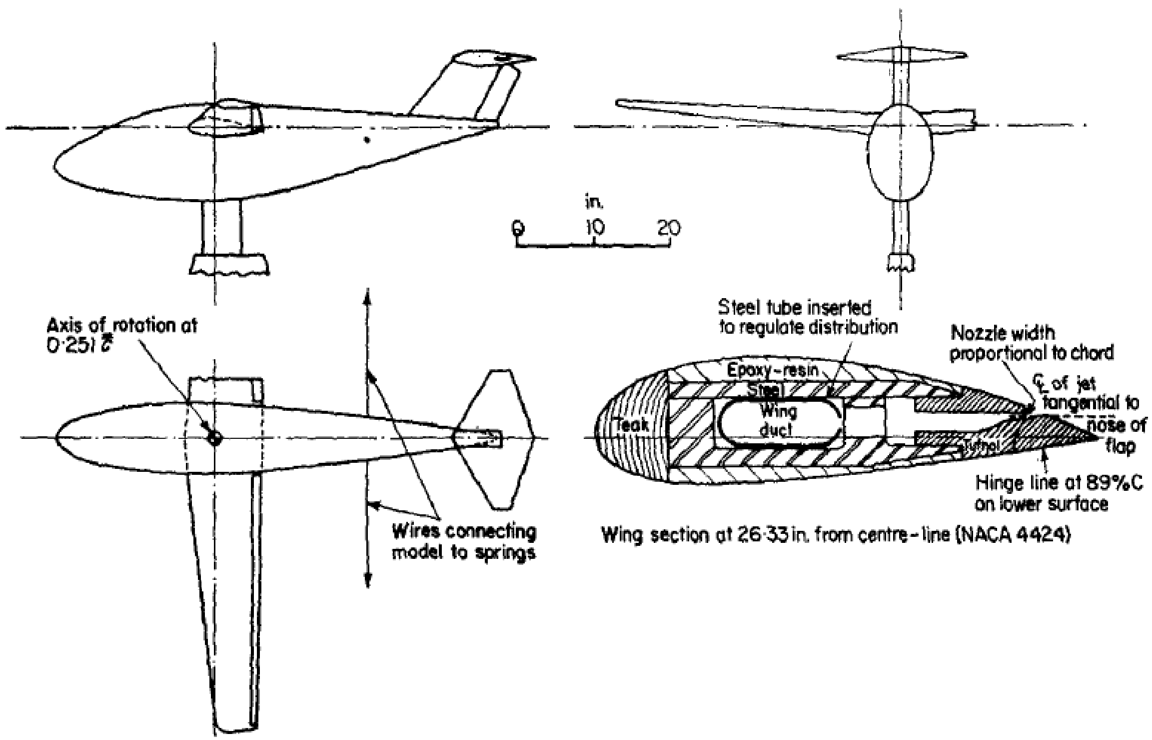

Manual Procedure

- The normal running procedure was as follows.
- (a) The blowing pressure corresponding to the desired value of C, was set.
- (b) The wind-tunnel speed was set at the prescribed value, and the spring attachment bolts were adjusted to remove any yaw on the model-t due to asymmetric thrust or aerodynamic moment.
- (c) With positive damping, the model was manually forced by pulling cyclically on one of the wire/spring junctions until the amplitude was greater than + 6”, when the model was carefully released and the recorder started.1 The run was continued until the oscillations had damped out completely or had reached a small, steady, residual amplitude.

Mechanical Design system balance

- Naturally, the problem of separating out the aerodynamic components of the yawing moment is eased if the inertia component can be cancelled, or very much reduced, and a simple angular accelerometer has been incorporated for this purpose.
- Strain-gauges on the leaf-springs are connected to give an output cancelling that obtained from the model yawing-moment balance due to the model inertia.
- The weights are adjusted wind-off to give approximate cancellation, leaving a small tare value which is measured at intervals to allow for drift due mainly to temperature.

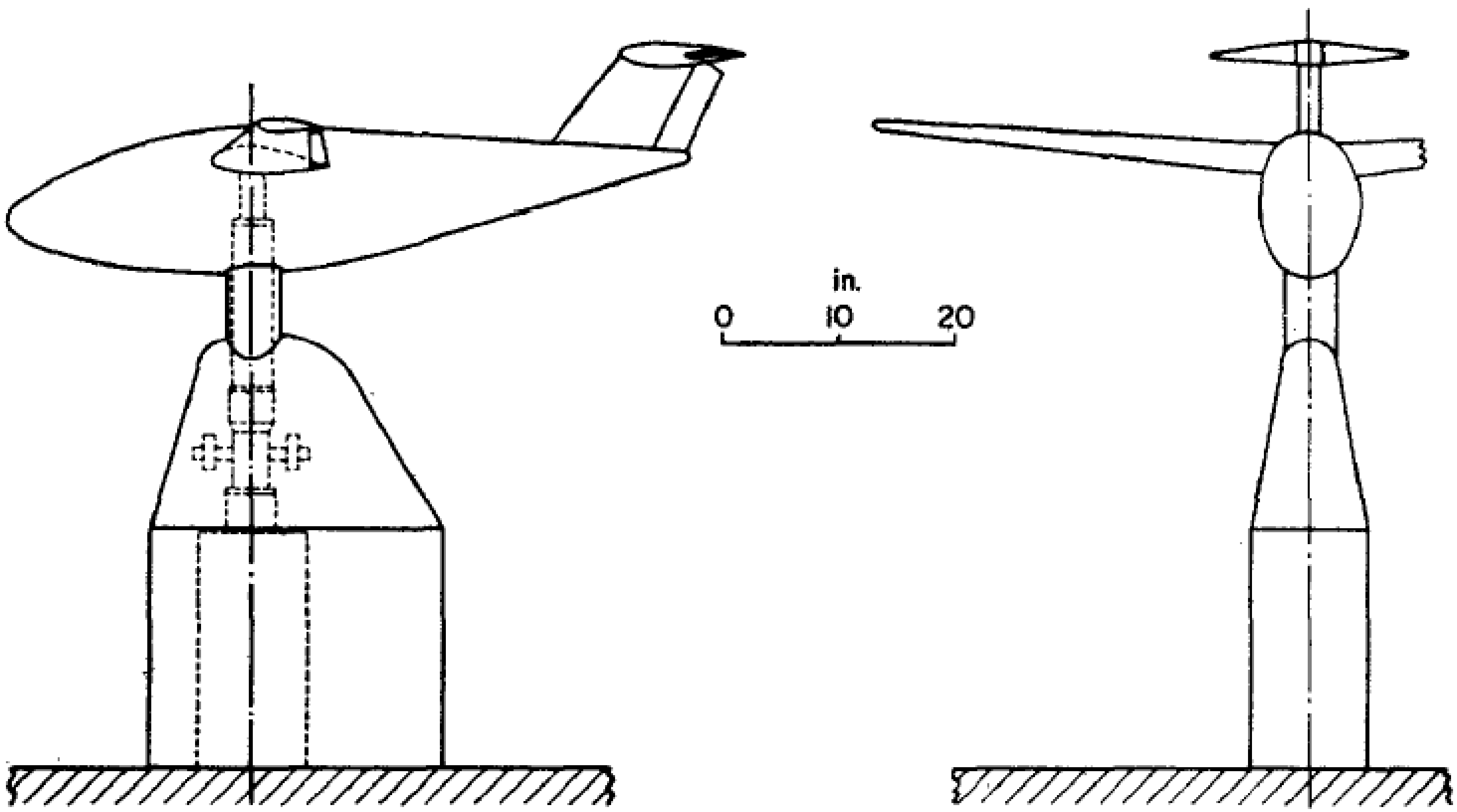

Jet-flap model on forced oscillation rig

Measurement of Pressure, Velocity and Temperature

Unit 4

Introduction

- Pressure measurement is important in many fluid mechanics related applications.
- From appropriate pressure measurements velocity, aerodynamic forces and moments can be determined. Pressure is measured by the force acting on unit area.
- Measuring devices usually indicate differential pressure i.e. in relation with atmospheric pressure. This is called gauge pressure.
- The measured pressure may be positive or negative with reference to the atmospheric pressure .A negative gauge pressure is referred to as vacuum.

Pressure

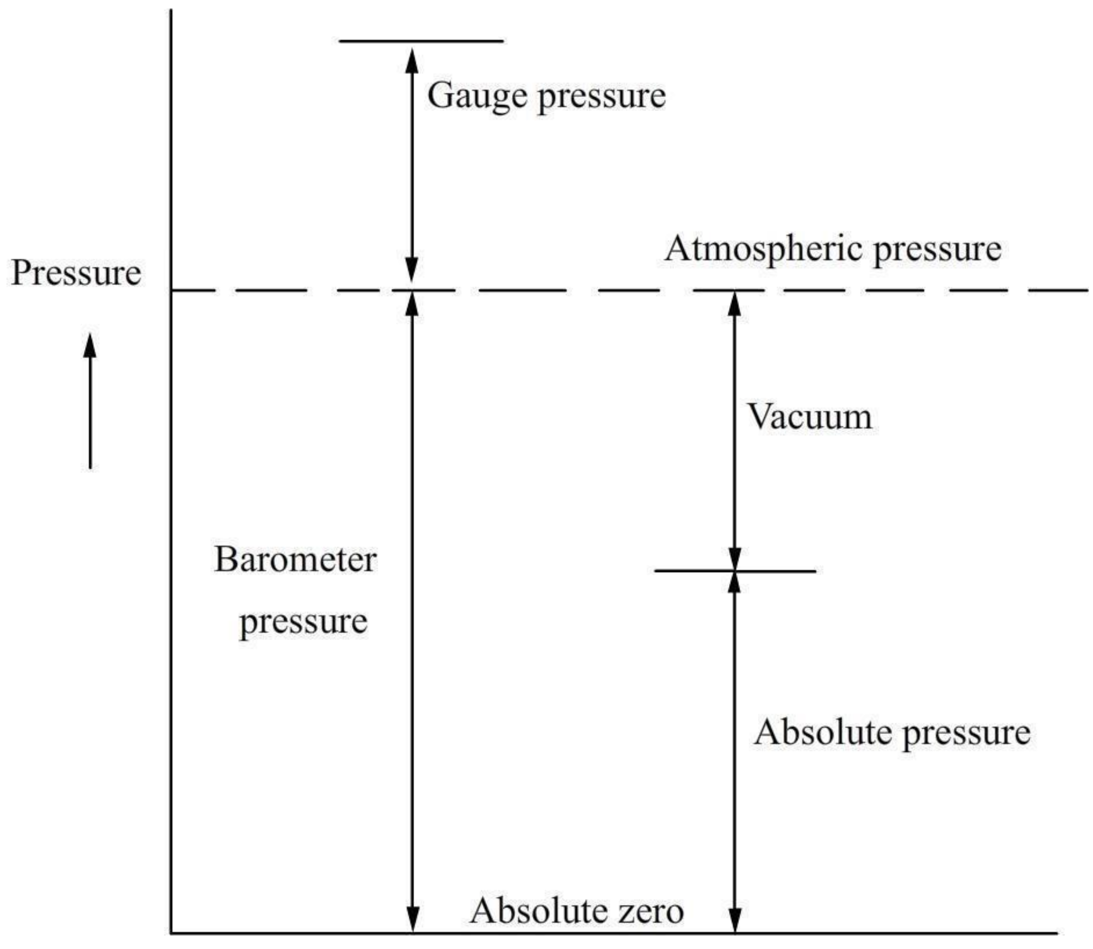
Gauge pressure
Atmospheric pressure
Pressure
Vacuum
Barometer
pressure
Absolute pressure
Absolute zero

Pressure measuring devices

- Liquid column manometers
- Pressure gauges with elastic sensing elements
- Pressure transducers
- Manometers for low absolute pressures
- Manometers for very high absolute pressures

Liquid column manometers

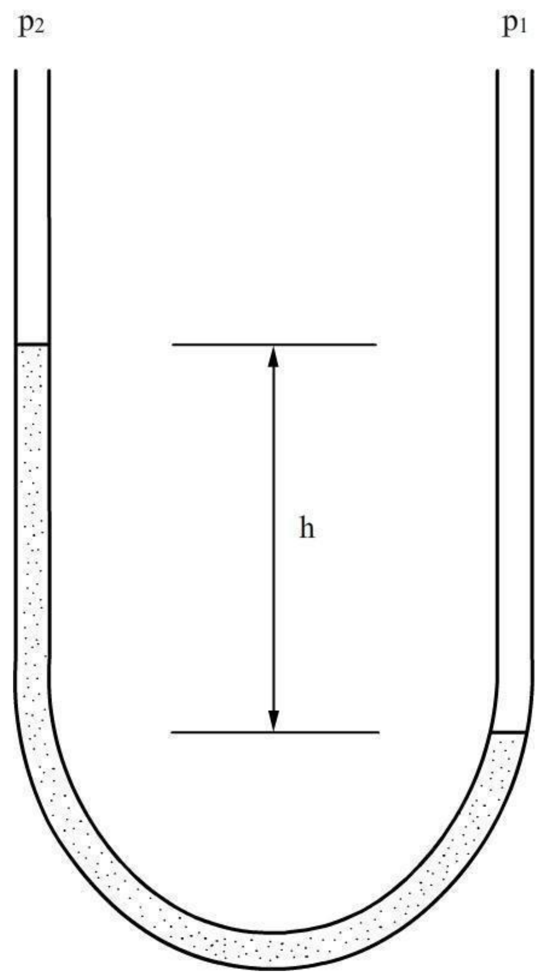

Inclined manometer

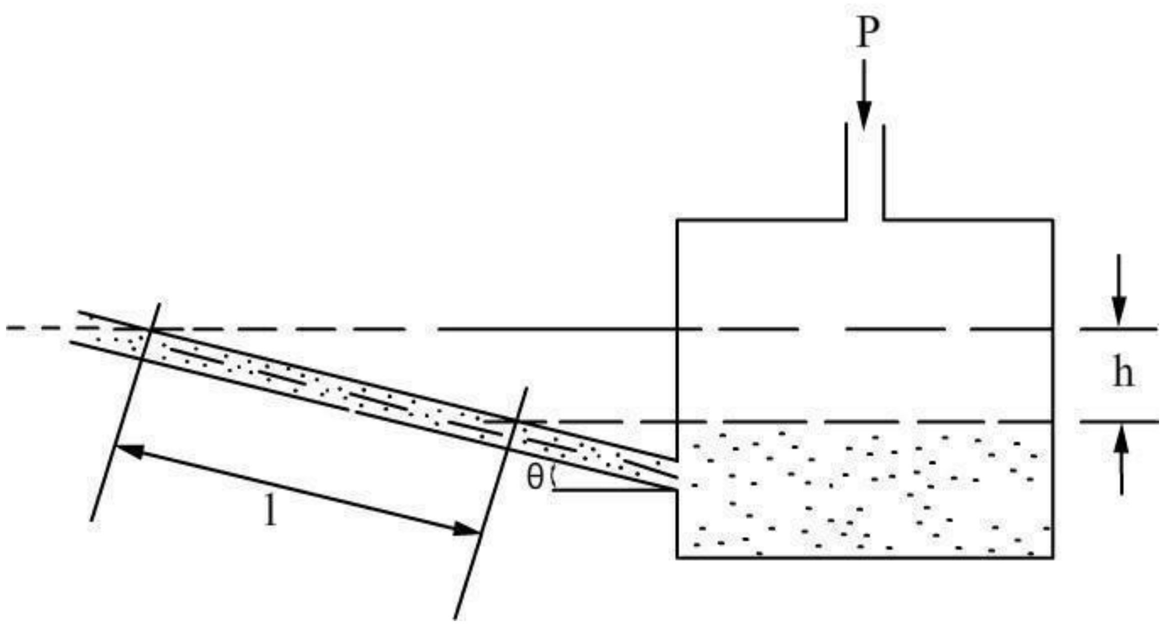

Inclined manometer

Mercury barometer

- Barometer is the device used to measure the atmospheric pressure.
- Mercury barometer consists essentially of a glass tube sealed at one end and mounted vertically in a bowl or cistern of mercury so that the open end of the tube is submerged below the surface of mercury in the cistern.

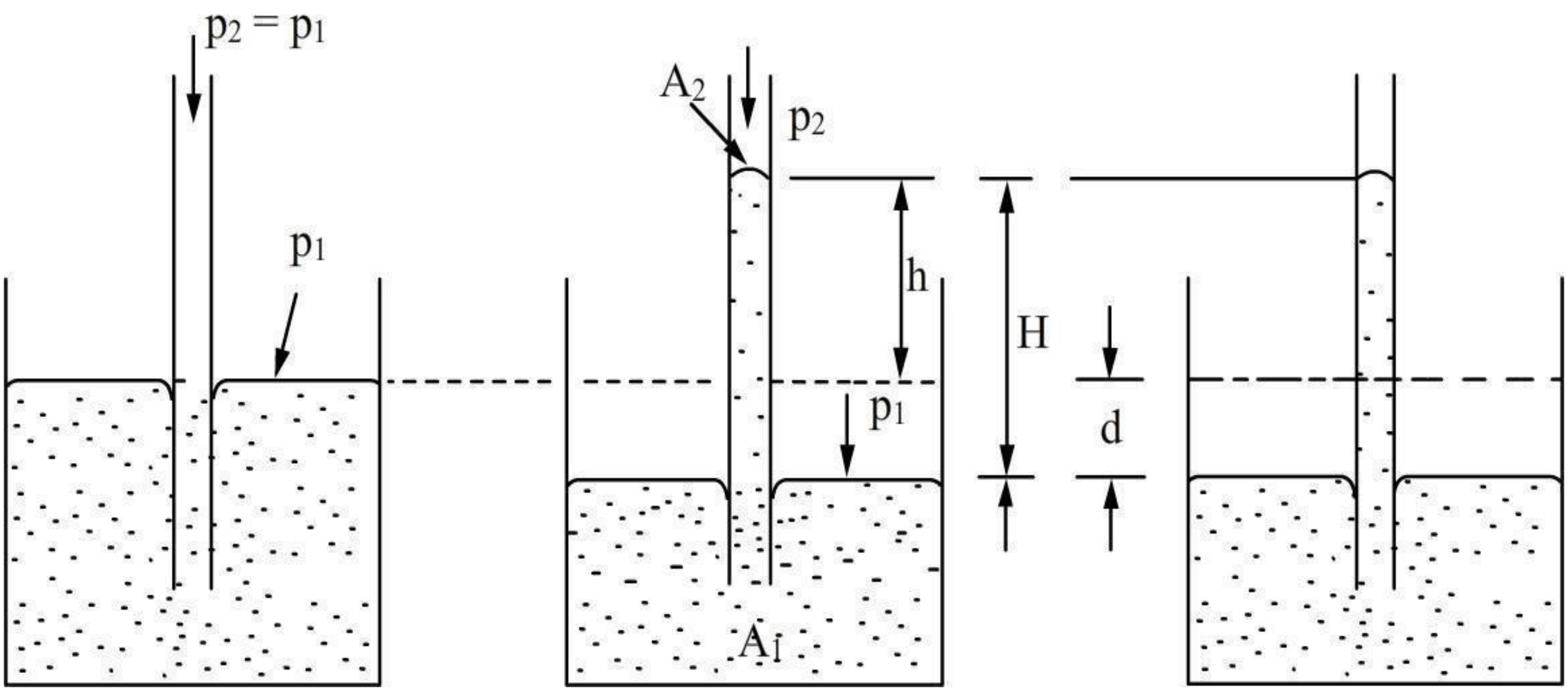

Principle of mercury barometer

Micro manometer

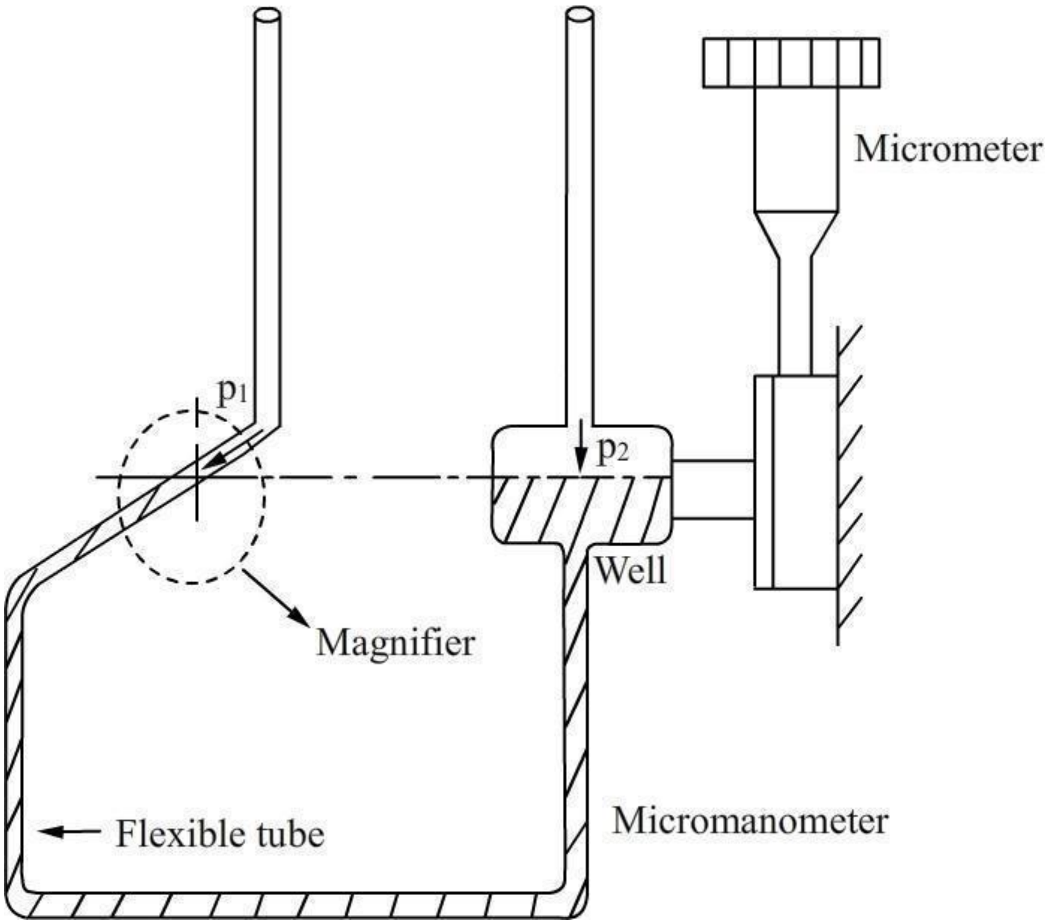

Mechanical manometers

- **Bourdon tube**
- **Elastic diaphragms**
- **Corrugated diaphragms**
- **Capsules, Bellows**

Lag in manometric systems

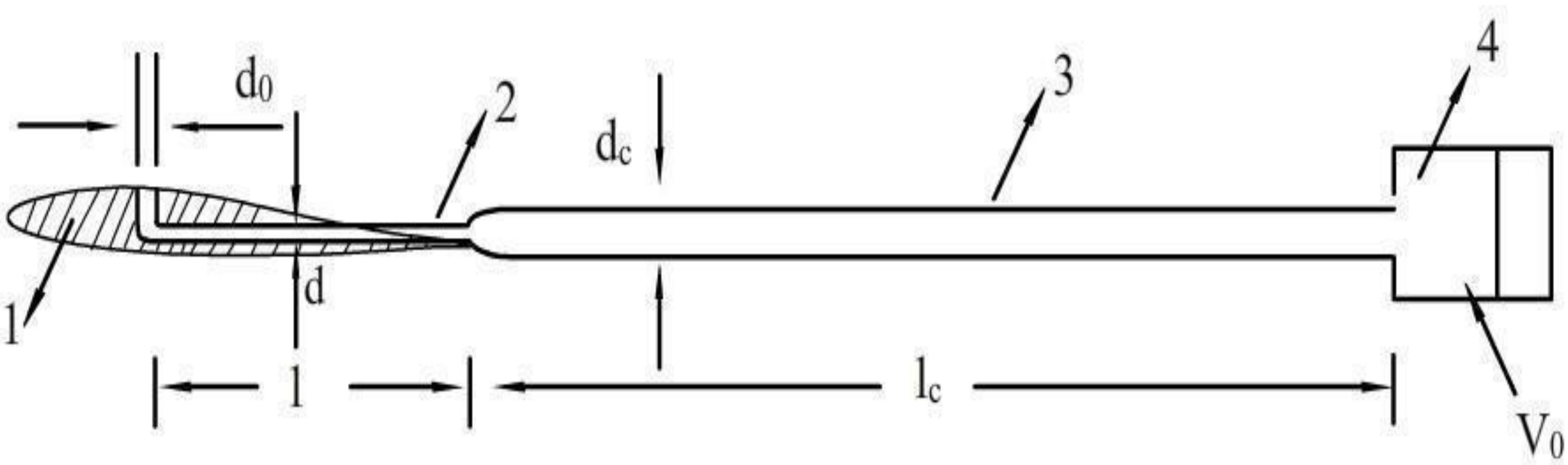

1 - model 2 - capillary tube 3 - connecting tube

4 - air space of sensing element of manometer

Wind tunnel model with the manometric system

Flow Visualization

UNIT- V

Introduction

- The visualization of complex flows has played a uniquely important role in the improvement of our understanding of fluid dynamic phenomena.
- Flow visualization has been used to verify existing physical principles and has led to the discovery of numerous flow phenomena.
- In addition to obtaining qualitative global pictures of the flow the possibility of acquiring quantitative measurements without introducing probes that invariably disturb the flow has provided the necessary incentive for development of a large number of visualization techniques.
- The role of flow visualization in experimental fluid-mechanical research has been appraised many times, and a number of reviews or comprehensive descriptions, either of the whole field or particular applications, are available.

Overview

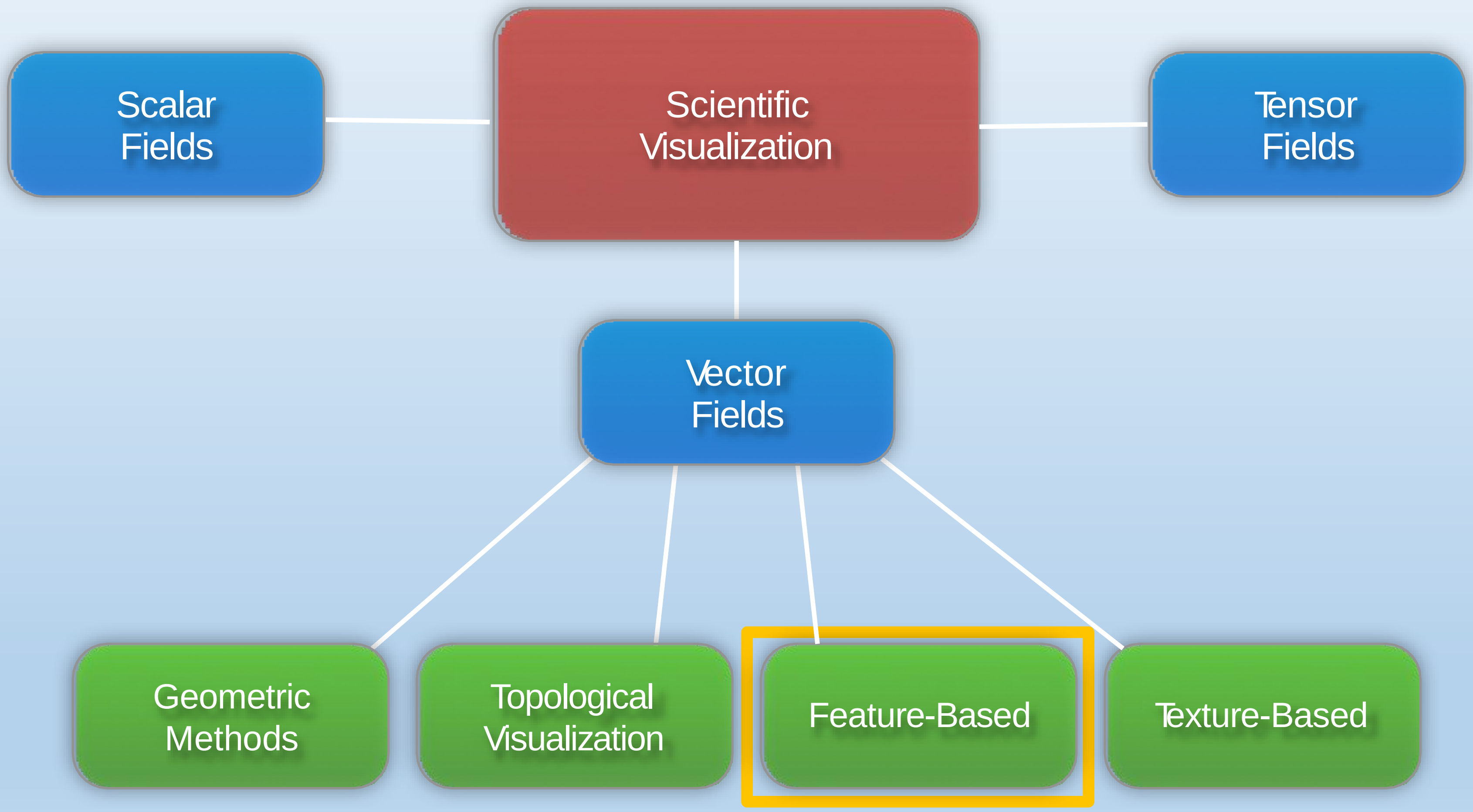

Scalar Fields
Scientific Visualization
Tensor Fields
Vector Fields
Geometric Methods
Topological Visualization
Feature-Based
Texture-Based

Flow Separation

- Flow abruptly leaves or returns to solid body (2D/3D phenomenon)
- Occurs along separation / attachment lines

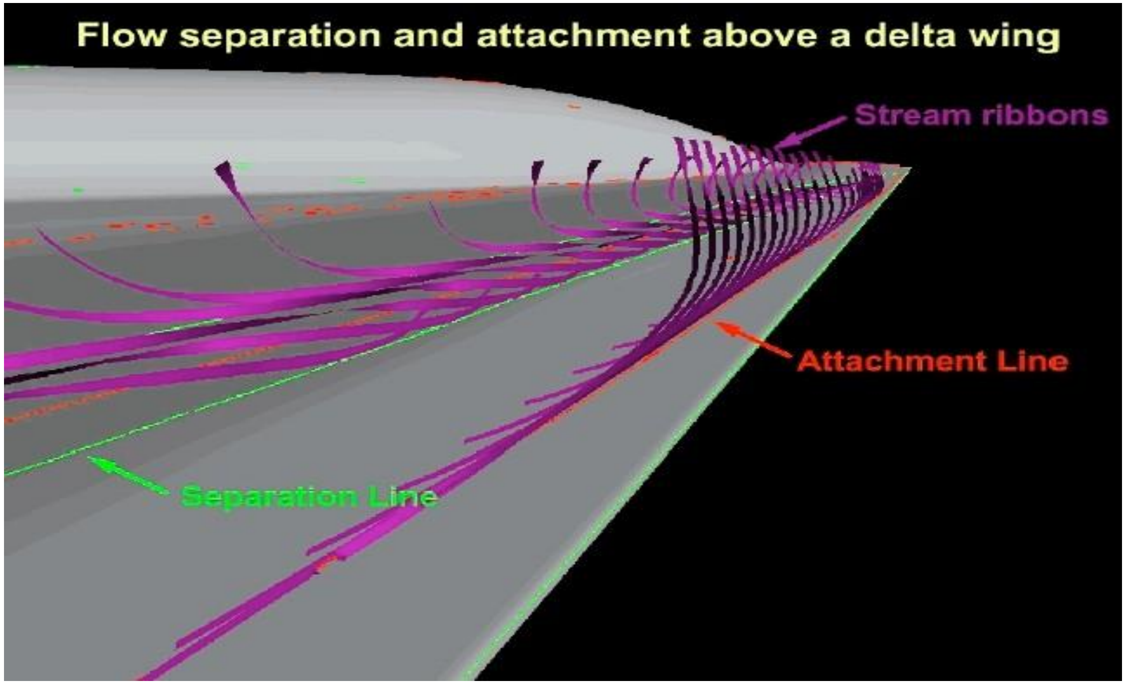

Flow Separation

- In 2D: separation and attachment points are critical points of tangential velocity

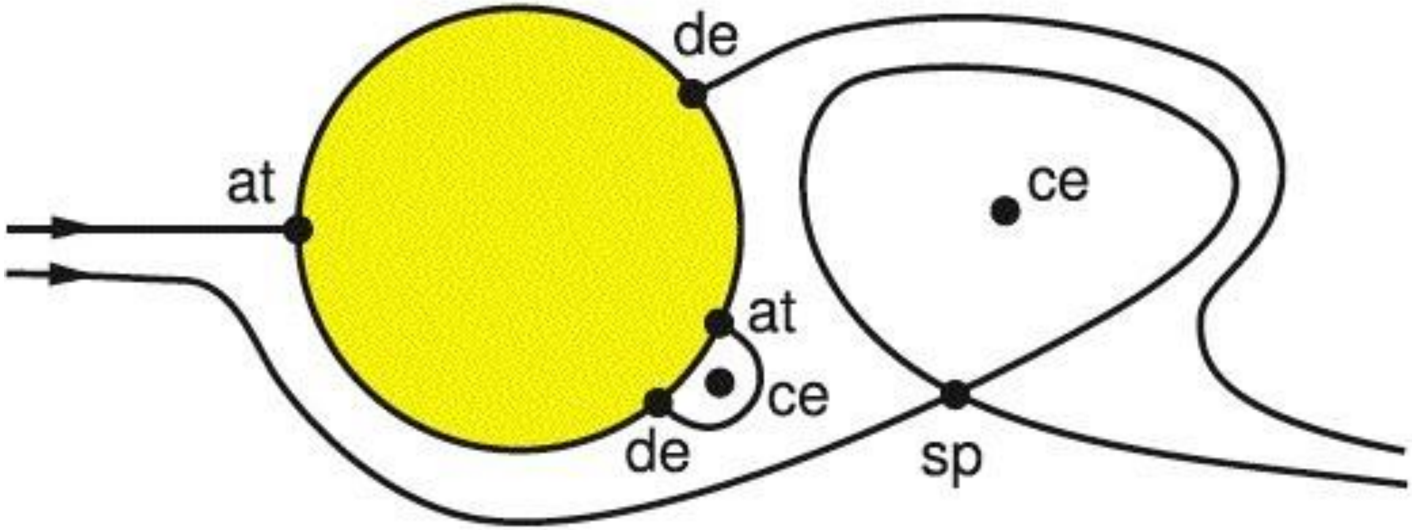

Topological Approach

- Work by Surana, Haller and others argue that flow separation is indeed a topological structure

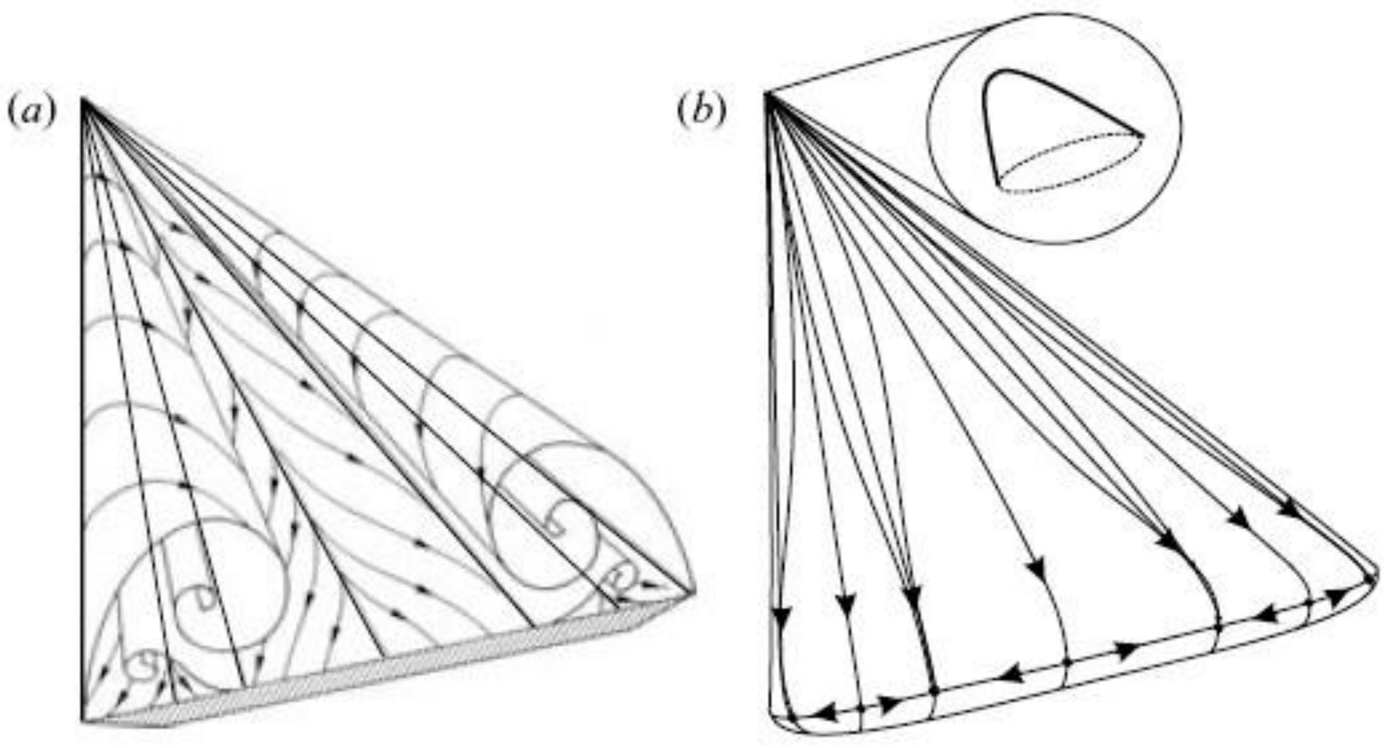

Flow Separation

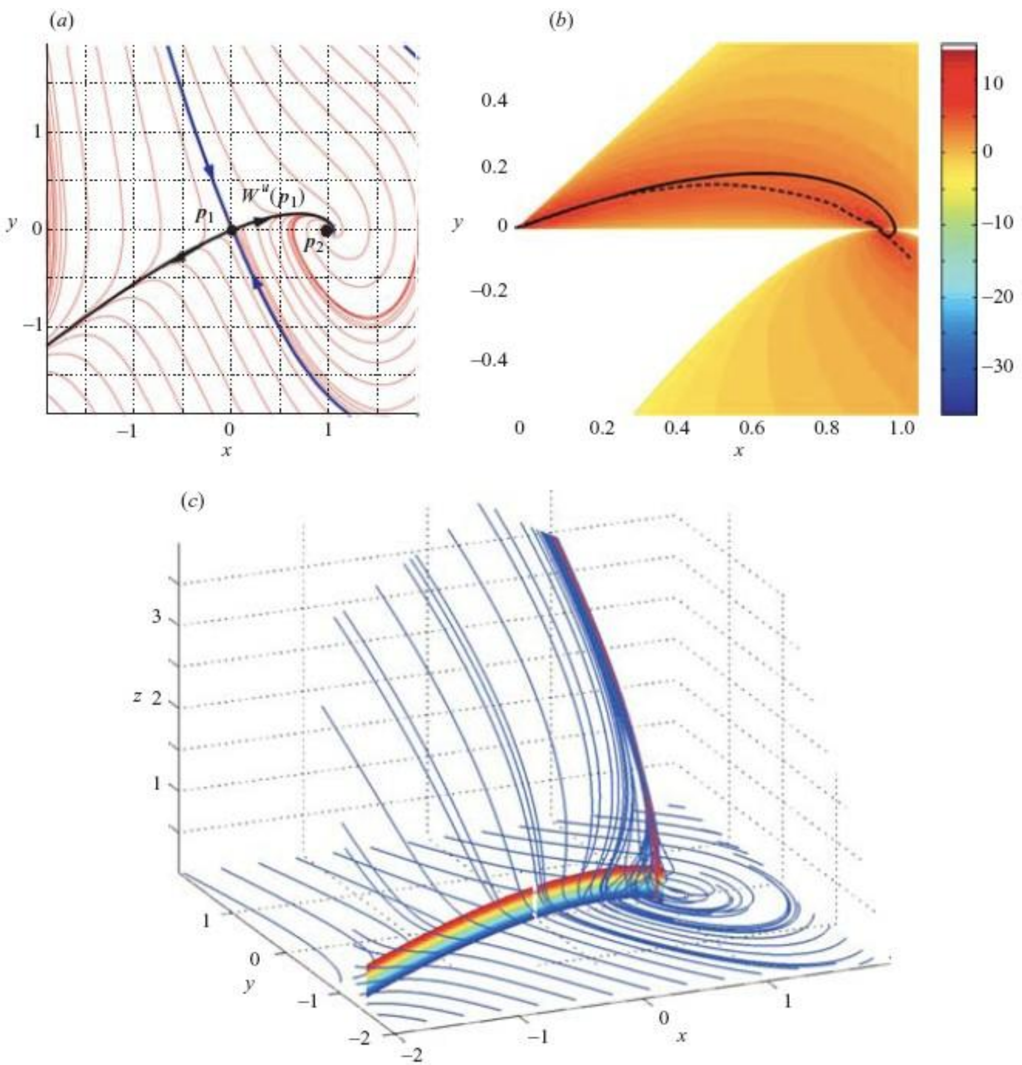

Flow Separation

- Superimposition of wall streamlines on oil flow patterns from experiment

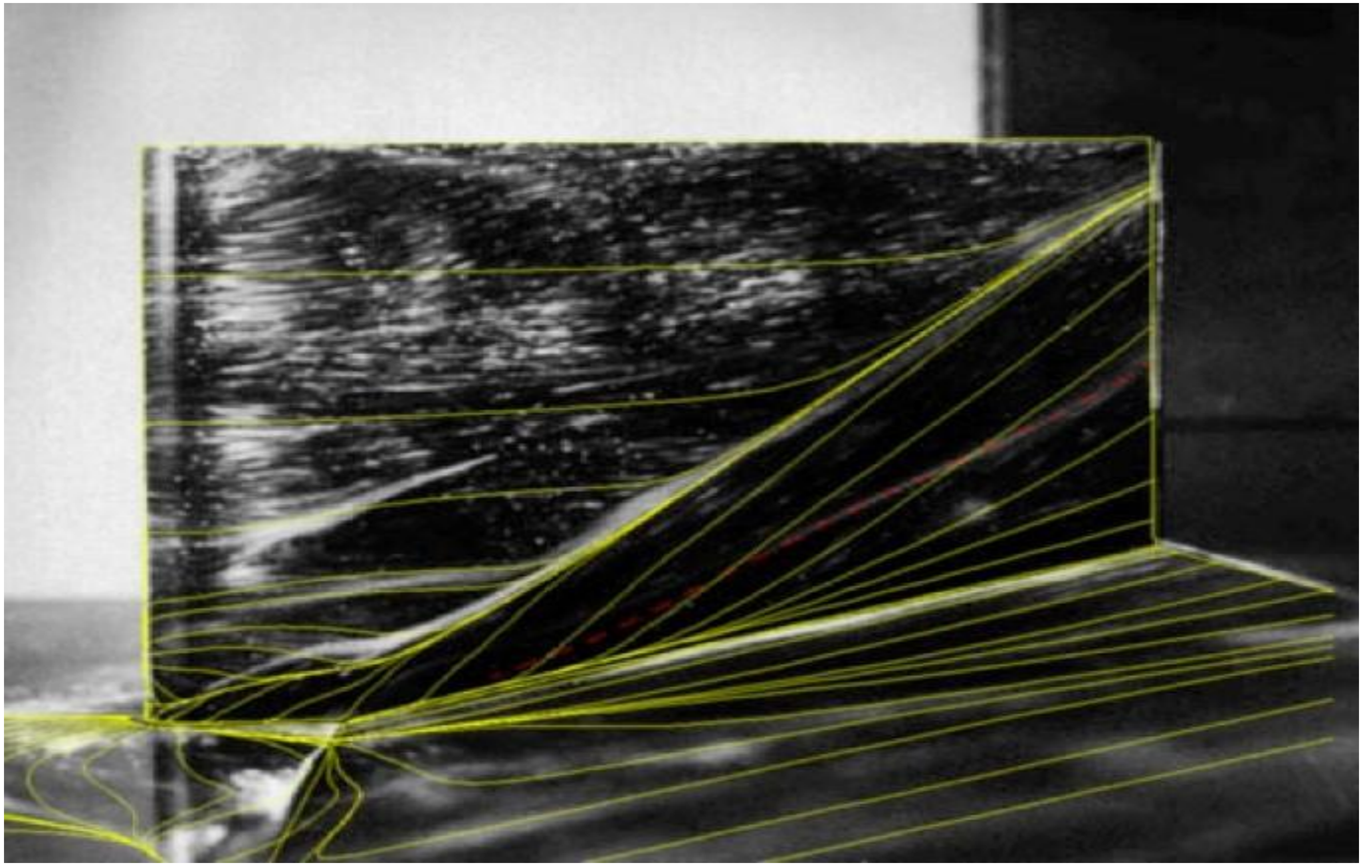

Flow Separation

- Kenwright's method: cell-wise pattern matching
  - Basic observation: separation / attachment lines present in two linear flow patterns

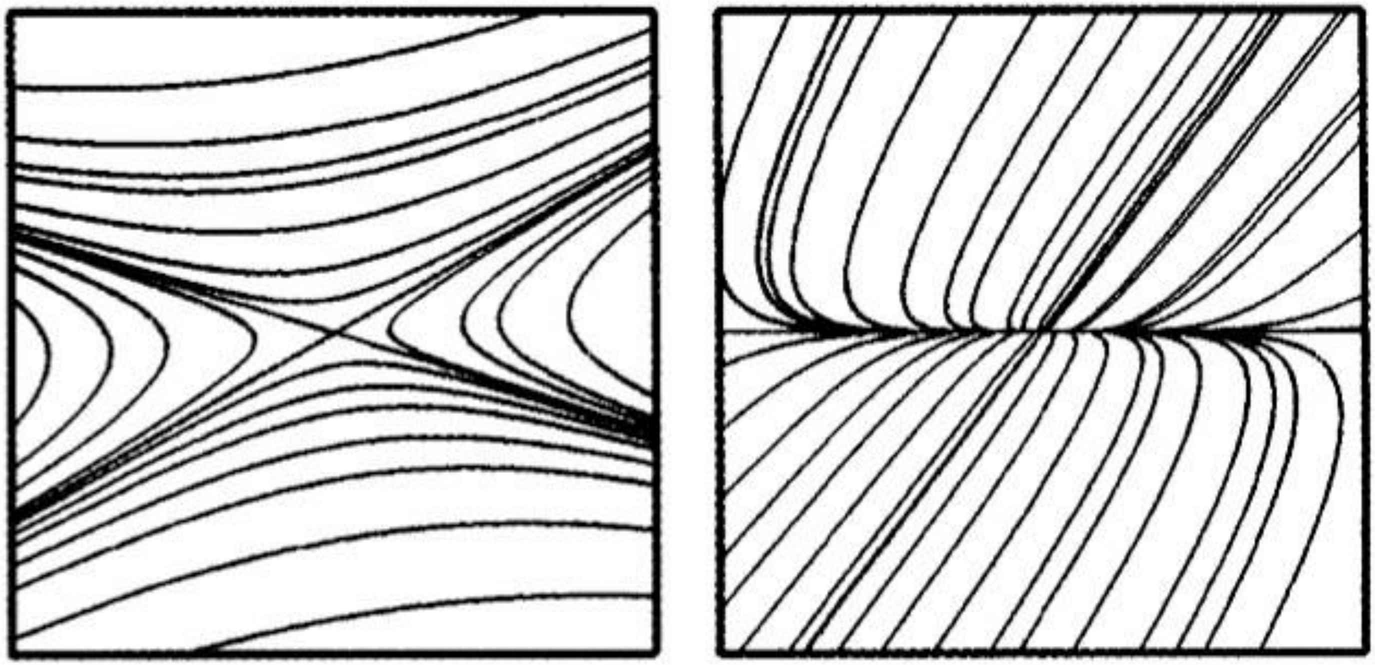

Flow Separation

- Kenwright's method: cell-wise pattern matching
  - Idea: extract intersection of those lines with each cell in piecewise linear flow

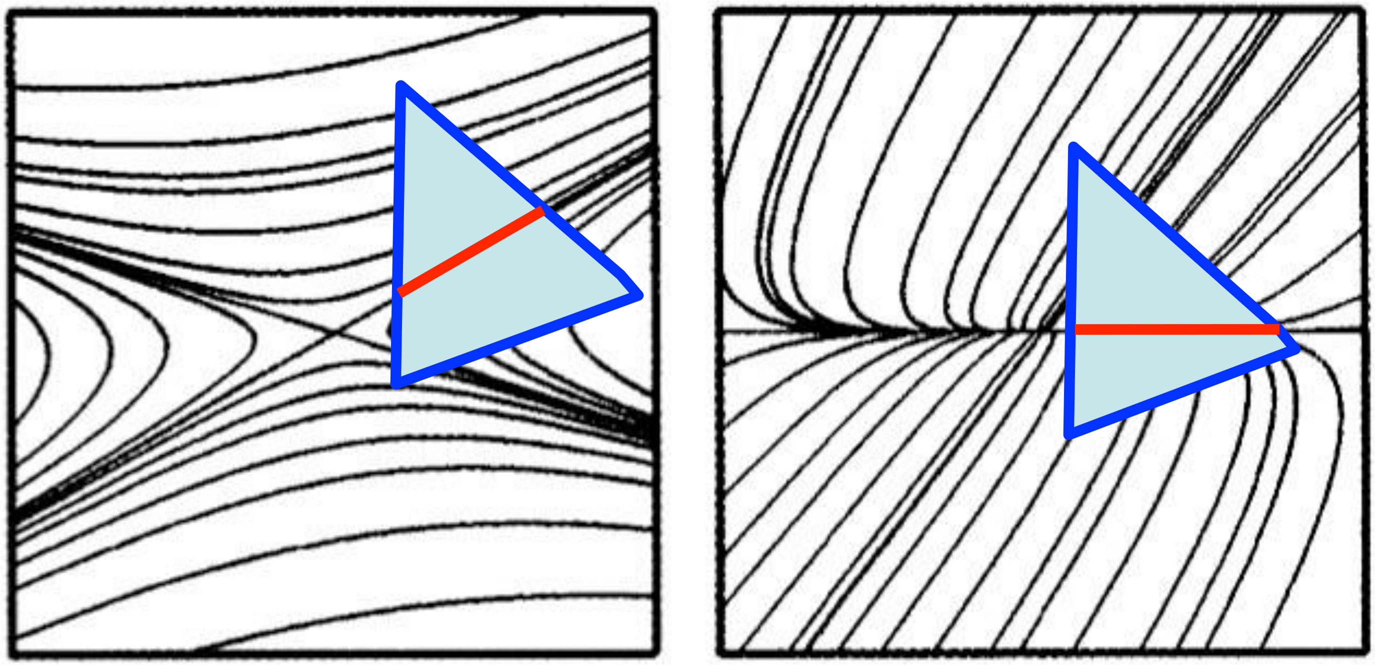

Flow Separation

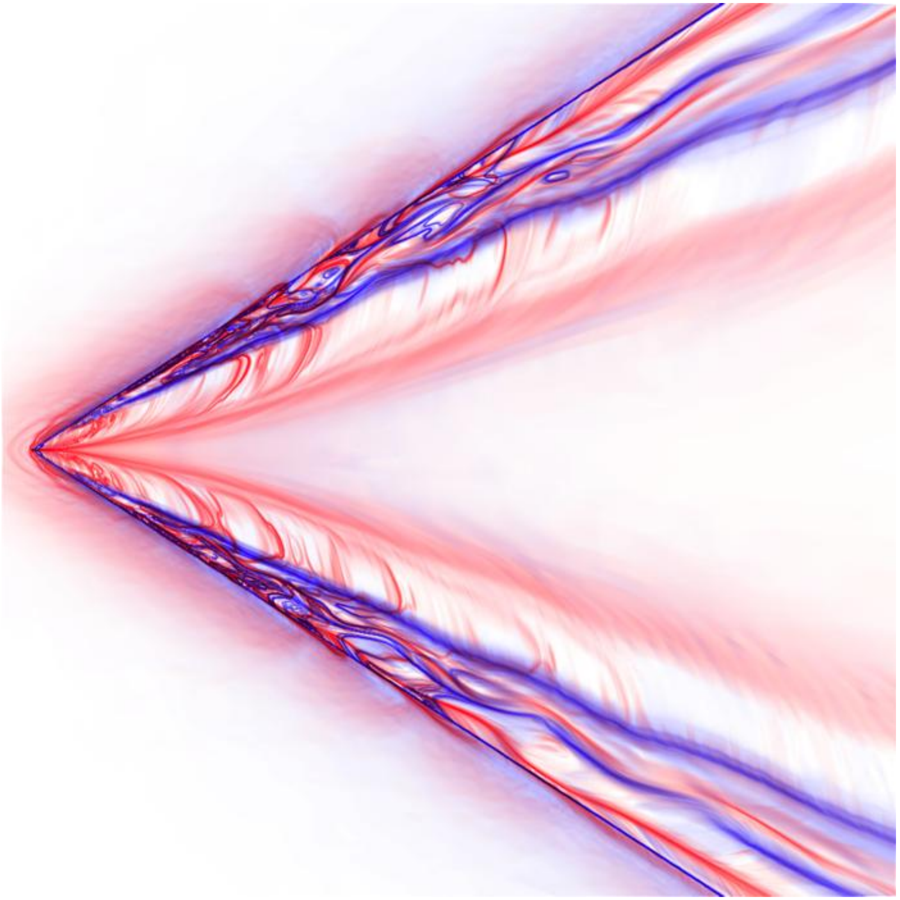

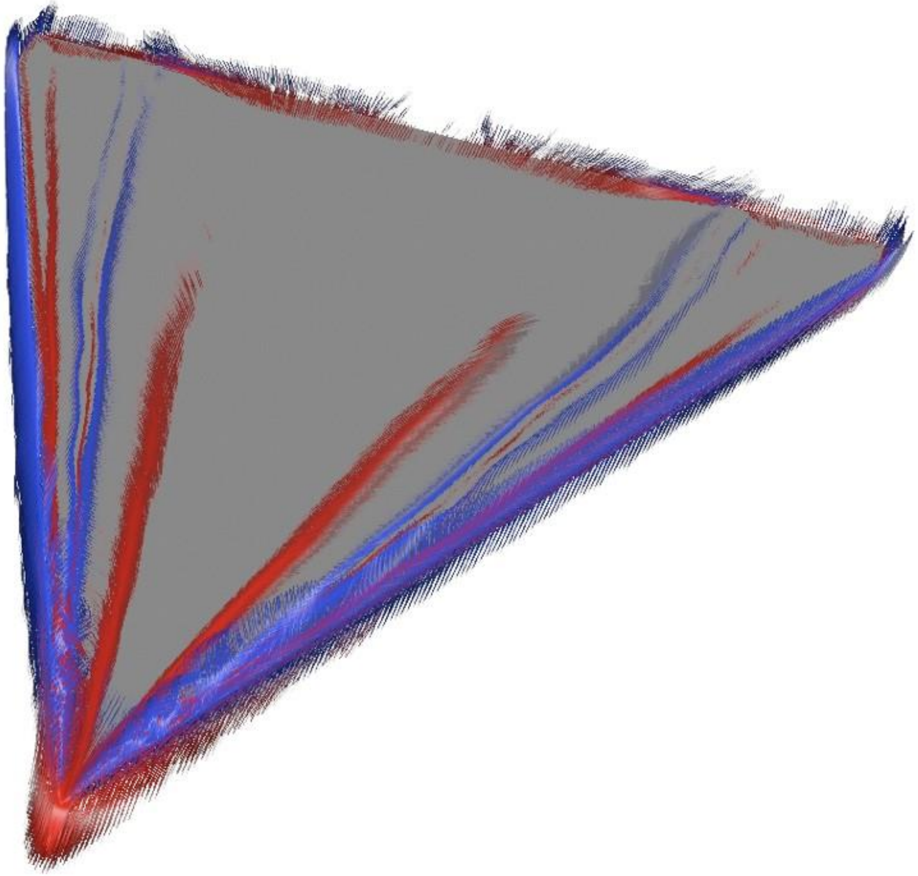

Flow Separation

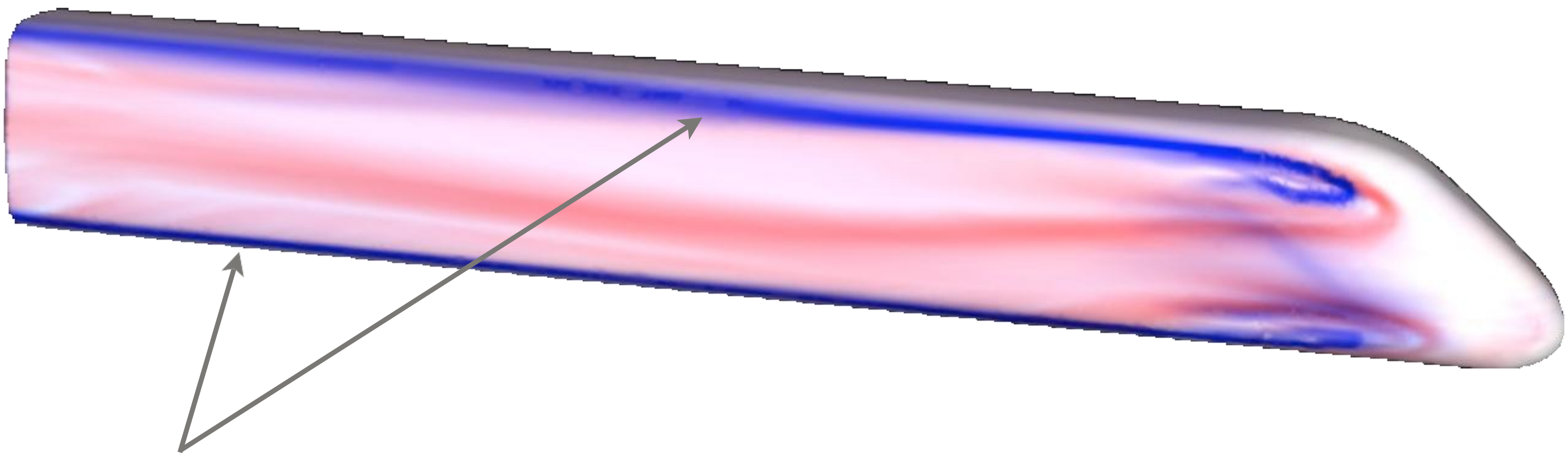

positive time FTLE^{+} (attachment)

negative time FTLE^{-} (separation)

Flow Separation

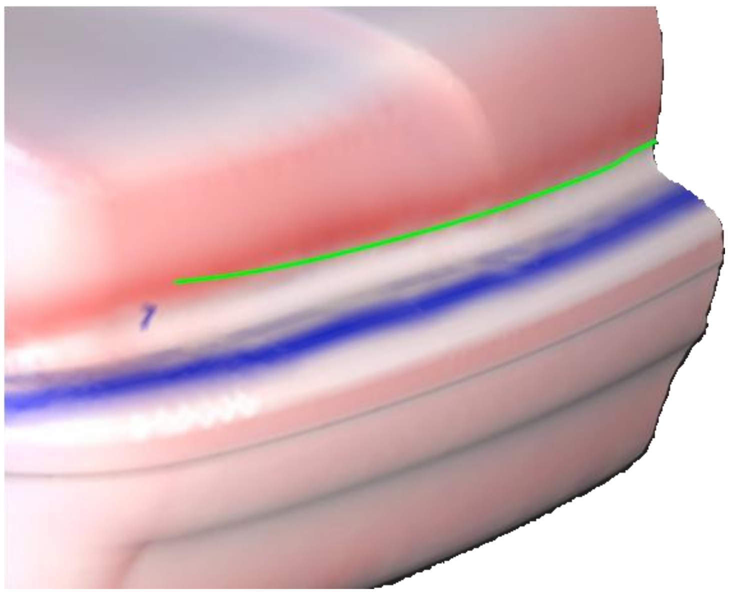

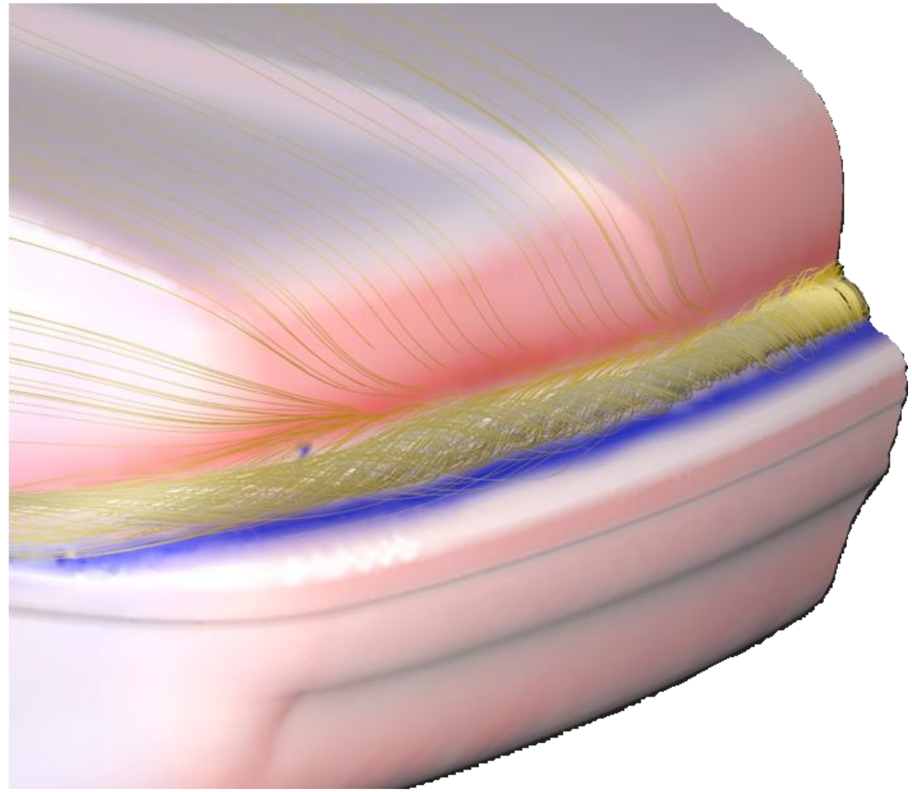

Overview

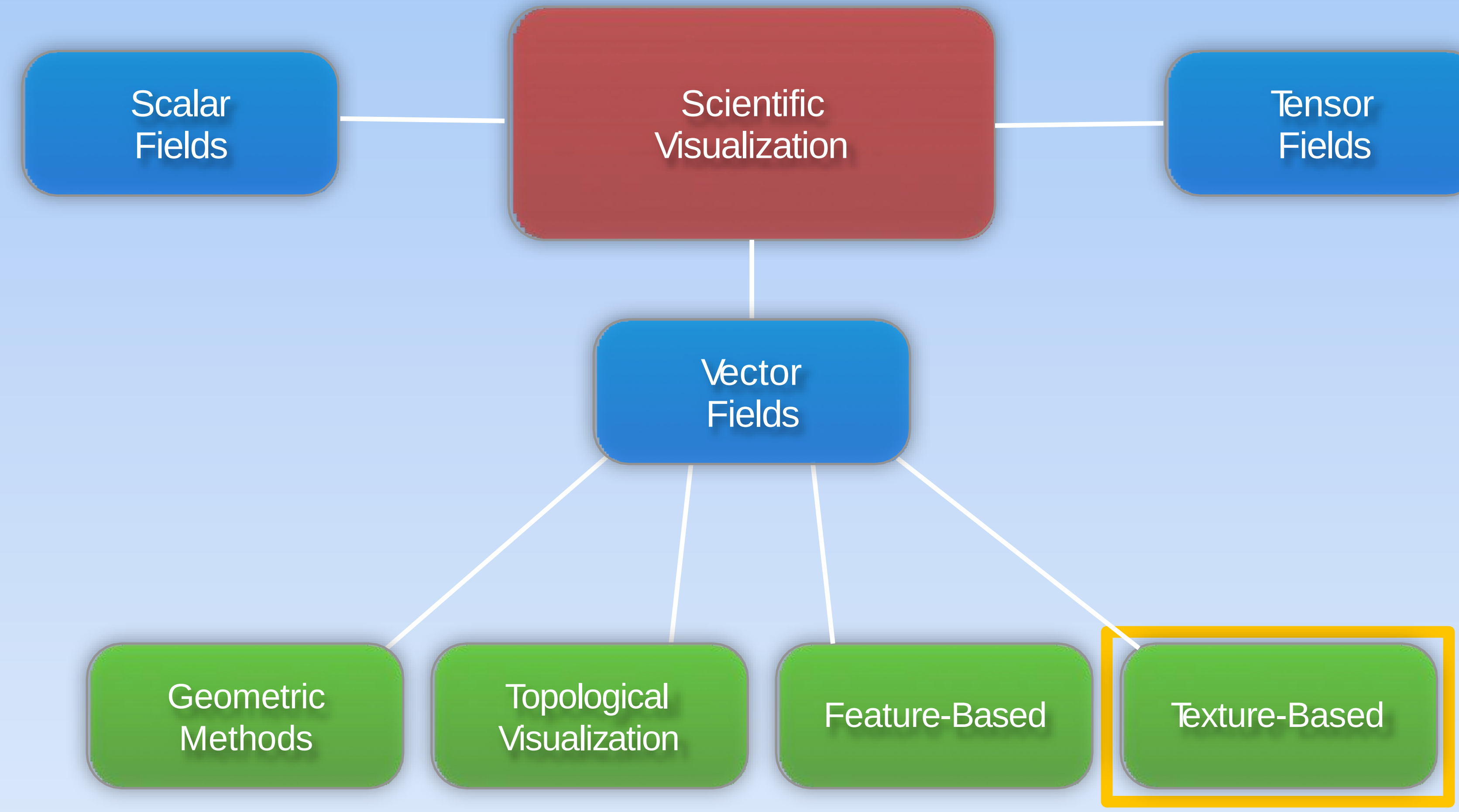
Scalar Fields
Scientific Visualization
Tensor Fields
Vector Fields
Geometric Methods
Topological Visualization
Feature-Based
Texture-Based

Spot Noise

- General technique for synthesis of stochastic textures
- Texture is characterized by function *f*

$$f(\mathbf{x}) = \sum_{i} a_i h(\mathbf{x} - \mathbf{x}_i)$$

Scaling factor (random)

Spot function with local support

Random position

- Spots of random intensity drawn and blended at random positions

Spot Noise

- Shape of the spot determines nature of the texture

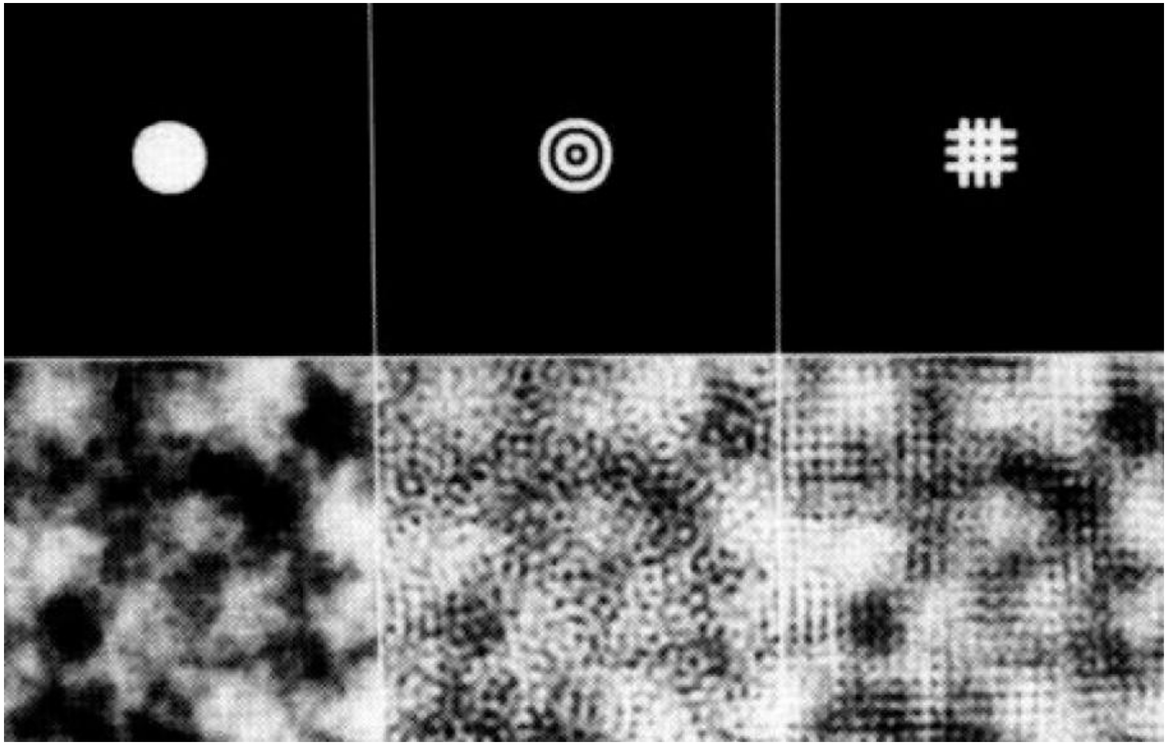

J. van Wijk, Spot Noise, Texture Synthesis for Data Visualization,
ACM SIGGRAPH '91

Spot Noise

- Spot function allows for local control over texture: maps data value (vector) to spot

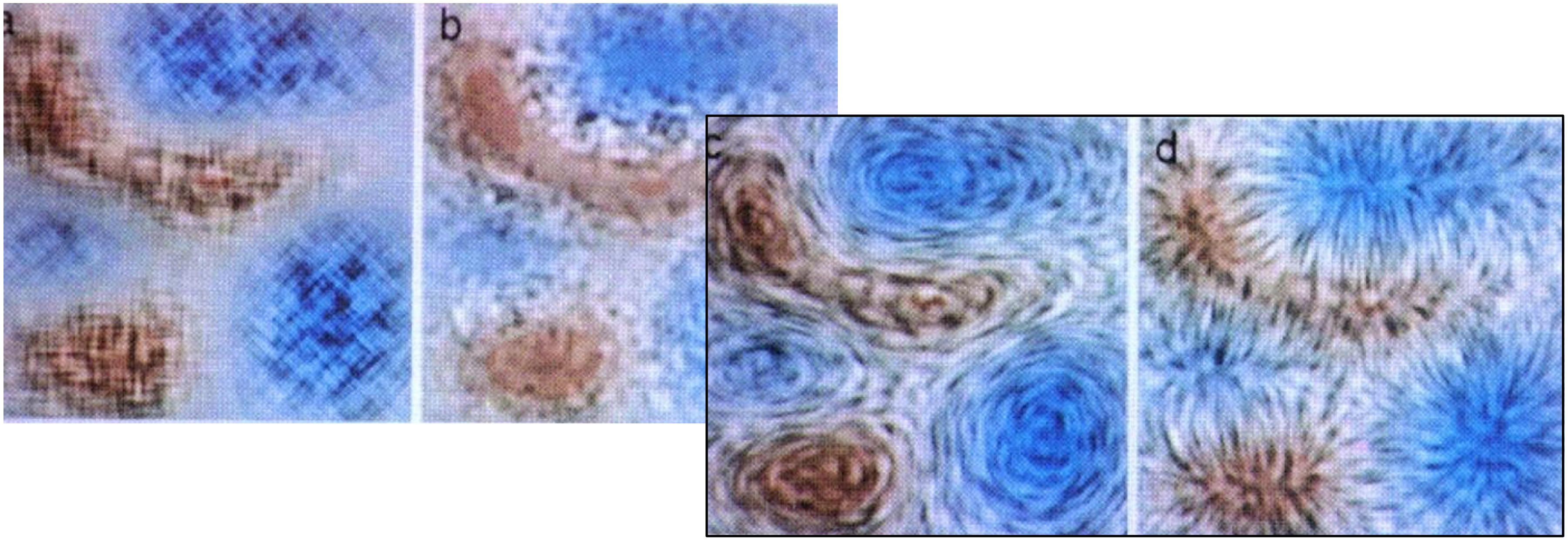

J. van Wijk, Spot Noise, Texture Synthesis for Data Visualization, ACM SIGGRAPH '91

Spot Noise

- Elliptical spots for visualizing 2D flows
  - Aligned with local flow direction
    - Long axis proportional to $v(\mathbf{x})$
    - Small axis proportional to $1/|v(\mathbf{x})|$
  - Orthogonal to flow direction (waves)

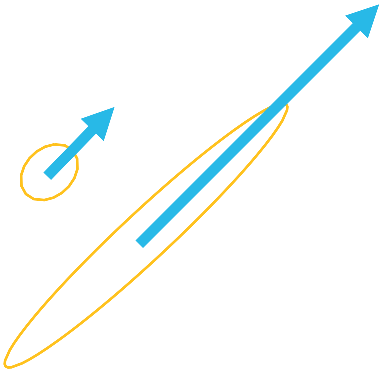

- Spot blending assumes local smoothness of underlying flow field

Spot Noise

- Animated Spot Noise for steady flow visualization:
  - Spots as moving particles
  - Over (fixed) lifetime
    - Appears
    - Moves along flow
    - Decays
  - Insertion position
  - Insertion time
  - Max intensity

Enhanced Spot Noise

- Spot bending (high flow curvature)
- Account for convergence divergence
- Ensure constant surface for each spot
- Solution: locally integrate stream surface

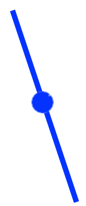

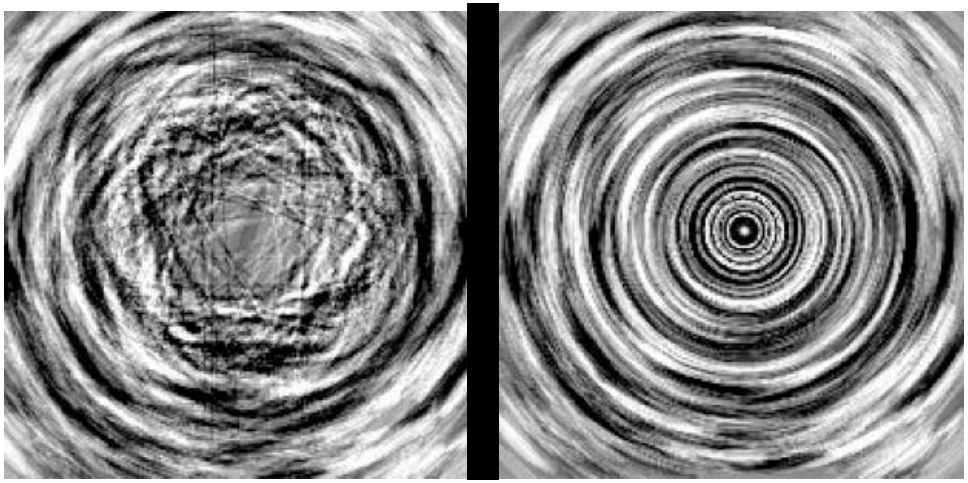

W. de Leeuw, J. van Wijk, Enhanced Spot Noise for Vector Visualization, IEEE Visualization ‘95

Enhanced Spot Noise

- Further improvements
  - High-pass spot filtering to increase texture homogeneity (avoid large light/dark regions)

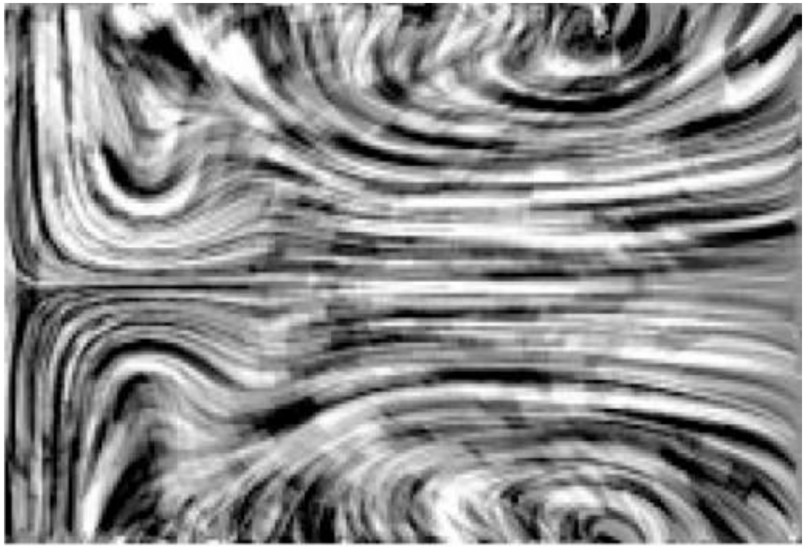

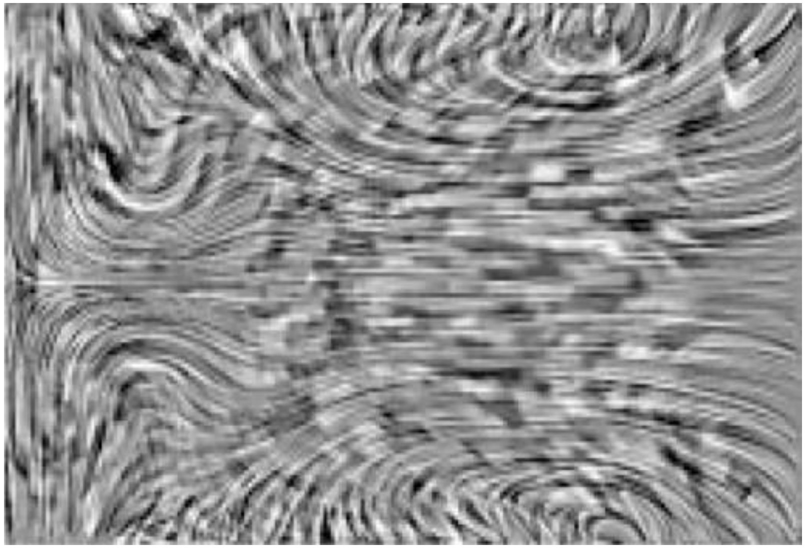

W. de Leeuw, J. van Wijk, Enhanced Spot Noise for Vector Visualization, IEEE Visualization ‘95

Enhanced Spot Noise

- Results

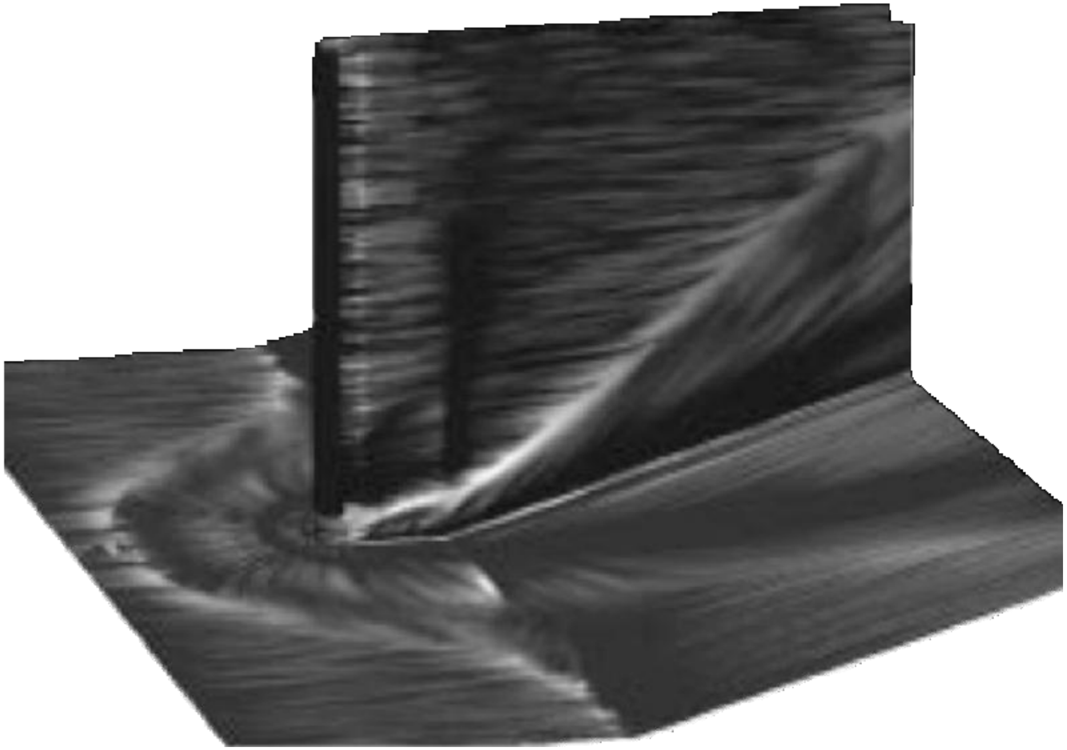

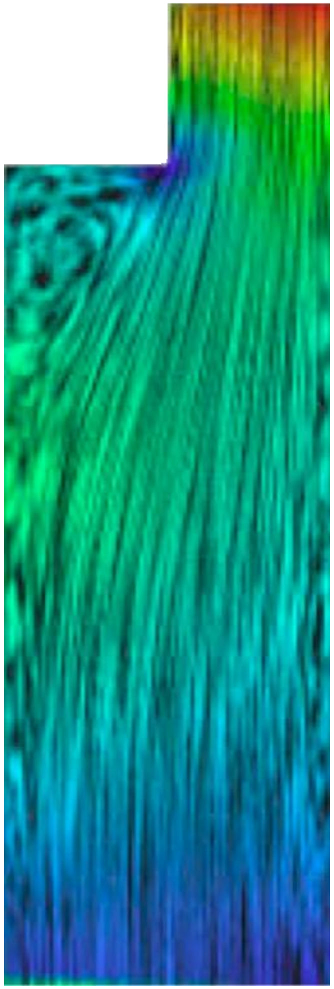

W. de Leeuw, J. van Wijk, Enhanced Spot Noise for Vector Visualization, IEEE Visualization ‘95

Line Integral Convolution

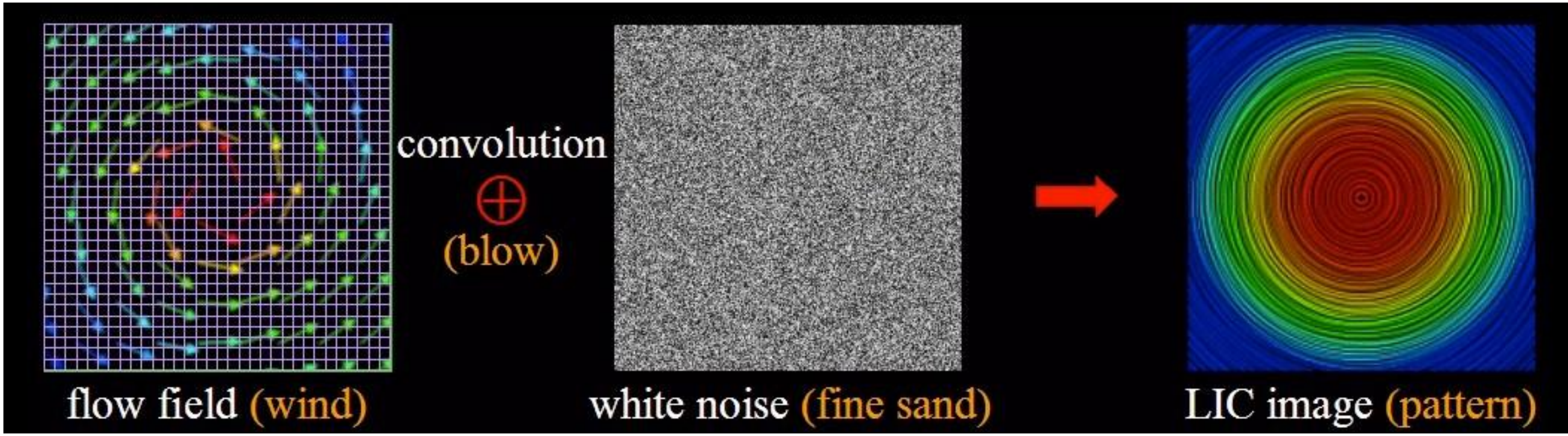

Line Integral Convolution

- Aliasing problems induced by white noise input texture can be solved by applying low pass filter (blurring) in pre-processing

- Simple convolution kernel: box

- Special convolution kernels can be used to show flow direction (periodic motion)

- Normalization applied after convolution to preserve brightness and contrast

Line Integral Convolution

- Correlation of pixels along the flow
- No correlation orthogonal to the flow
- Resulting pictures are similar to visualizations achieved with oil film applied onto surface of embedded body in wind tunnel experiments

B. Cabral, C. Leedom, Imaging Vector Fields Using Line Integral Convolution, ACM SIGGRAPH ‘93

Line Integral Convolution

- Results

Standard LIC

LIC

- Results

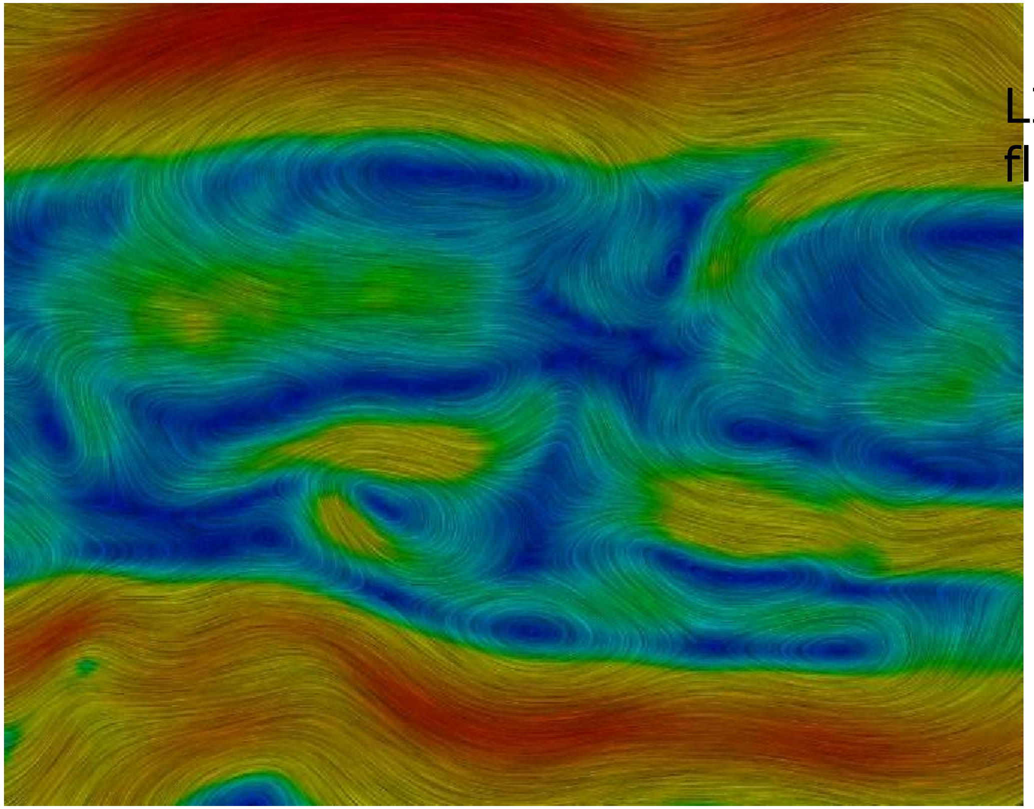

LIC + color coded
flow magnitude

LIC

- Results

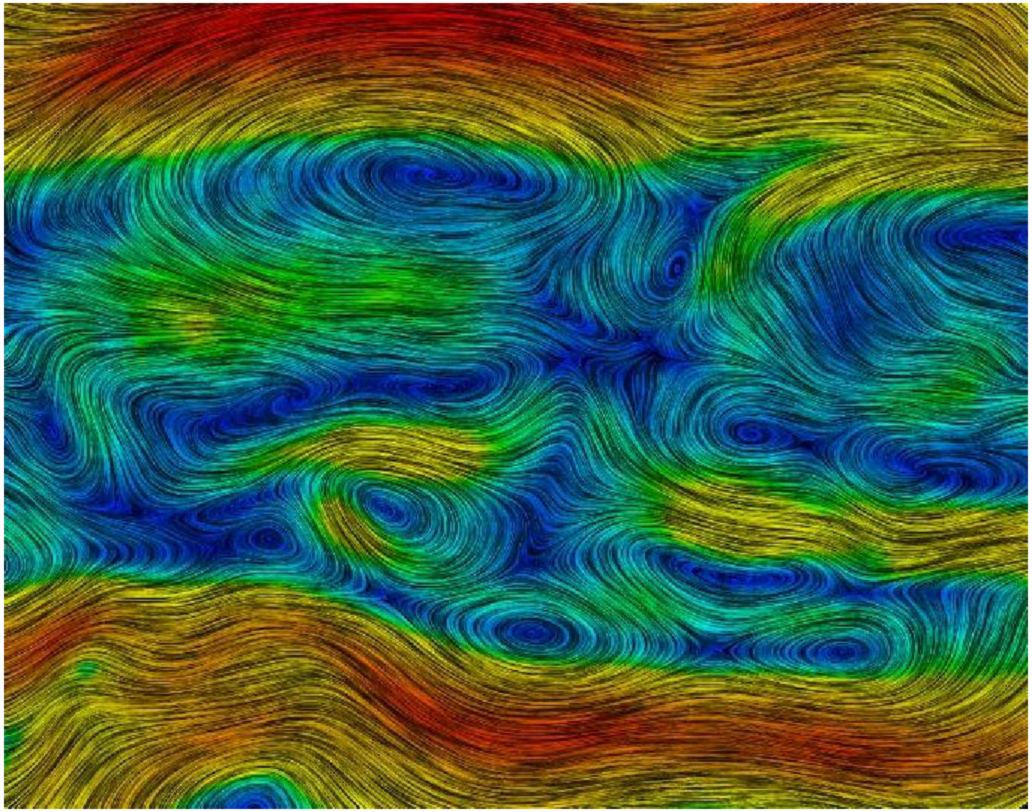

LIC

- Results

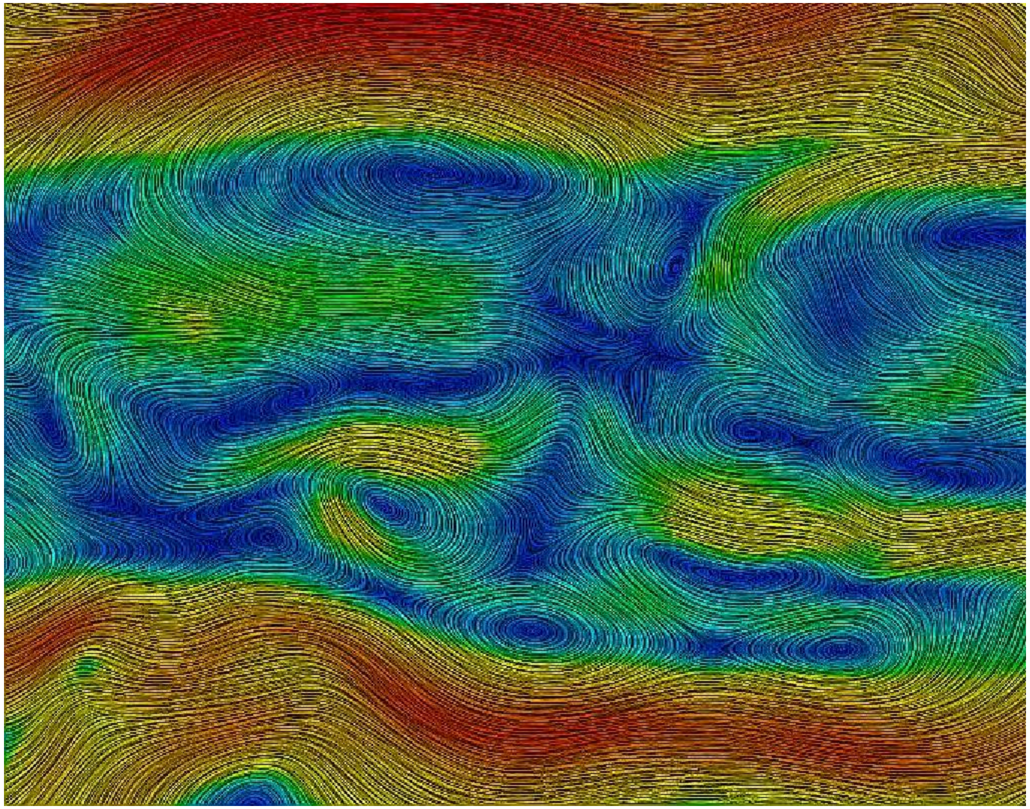

FastLI
C

- Exploit redundancy of streamlines covering many pixels
  - # streamlines is 2% of # pixels

- Use correlation between convolution coefficients

- Integrate flow using RK 45 + cubic interpolation

- 10x faster than standard LIC

D. Stalling, H.-C. Hege, Fast and Resolution Independent Line Integral Convolution, ACM SIGGRAPH ‘95

Enhanced LIC

- Improve contrast by iteratively taking last computed LIC texture as input for next iteration
- Combined with final high-pass filtering

A. Okada, D. L. Kao, Enhanced Line Integral Convolution and Feature Detection, IS & T / SPIE Electronics Imaging ‘97

Oriented LIC

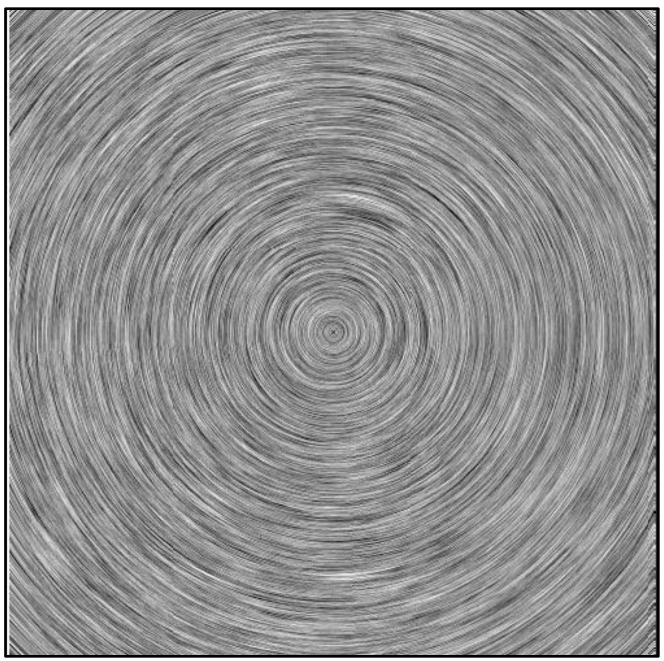

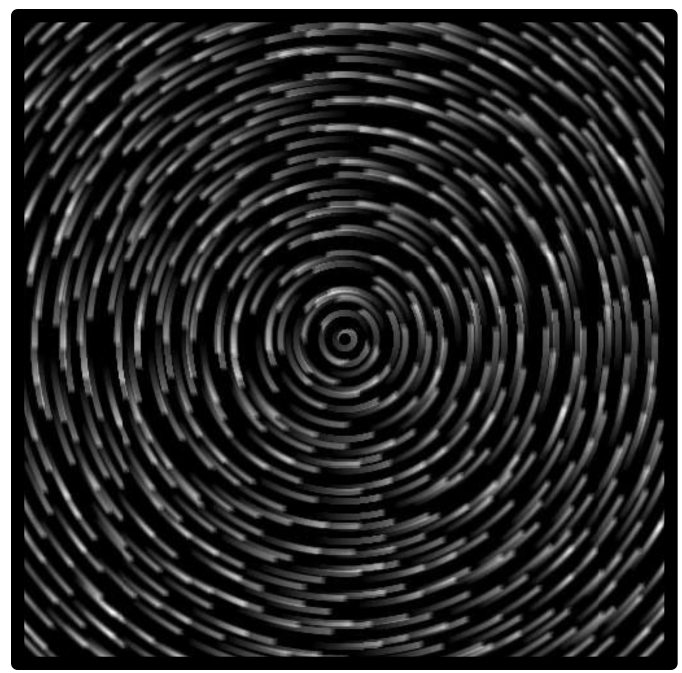

Multifrequency LIC

Kiu & Banks, Vis96

- Change frequency of noise texture image based on flow properties (e.g speed)

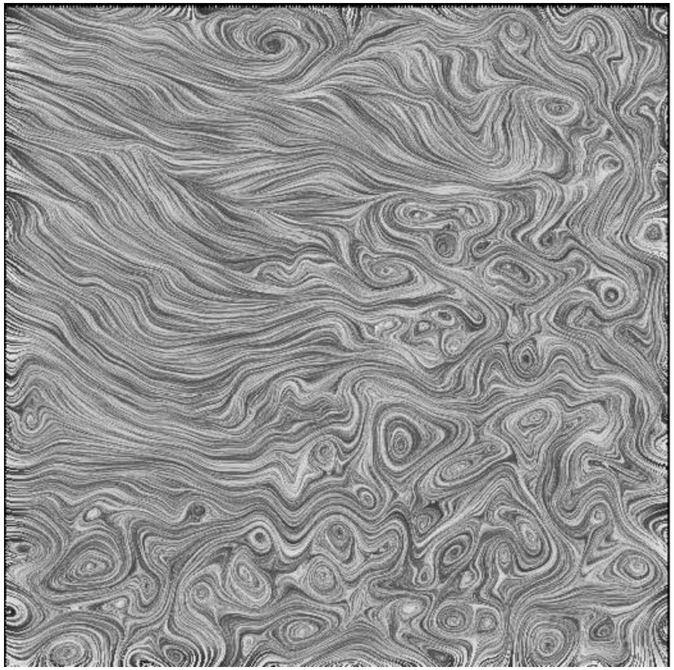

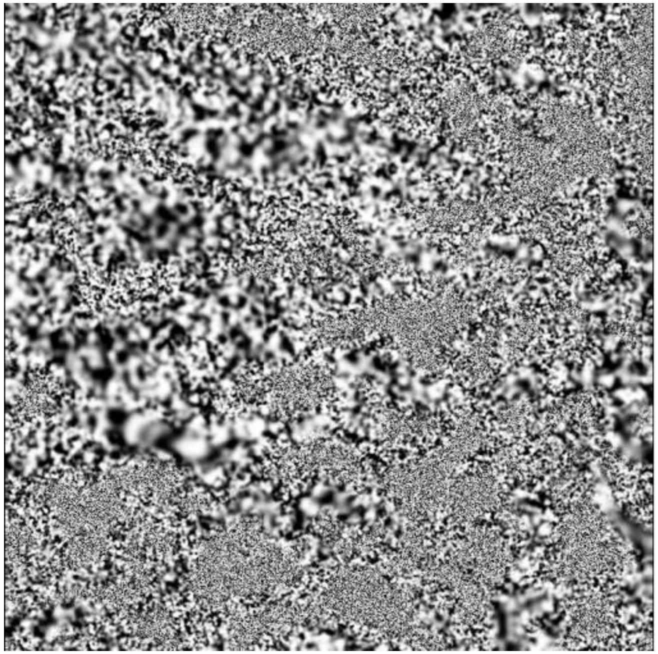

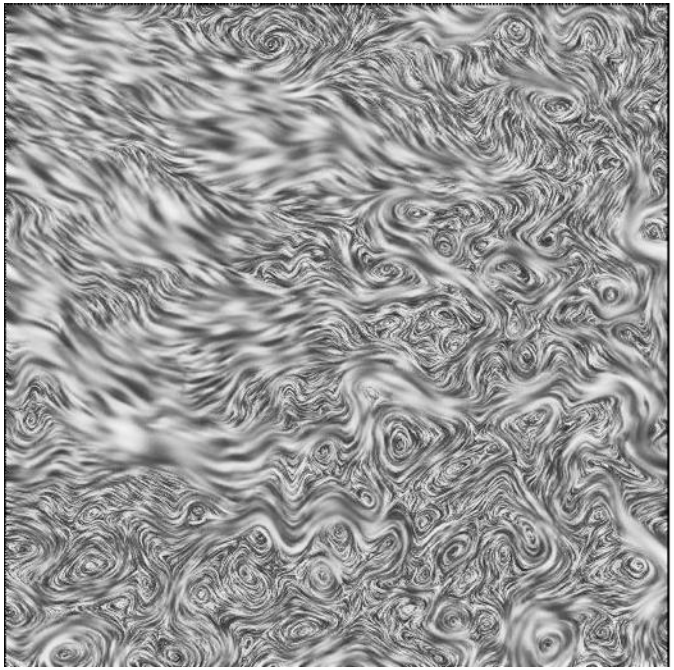

Moving Textures

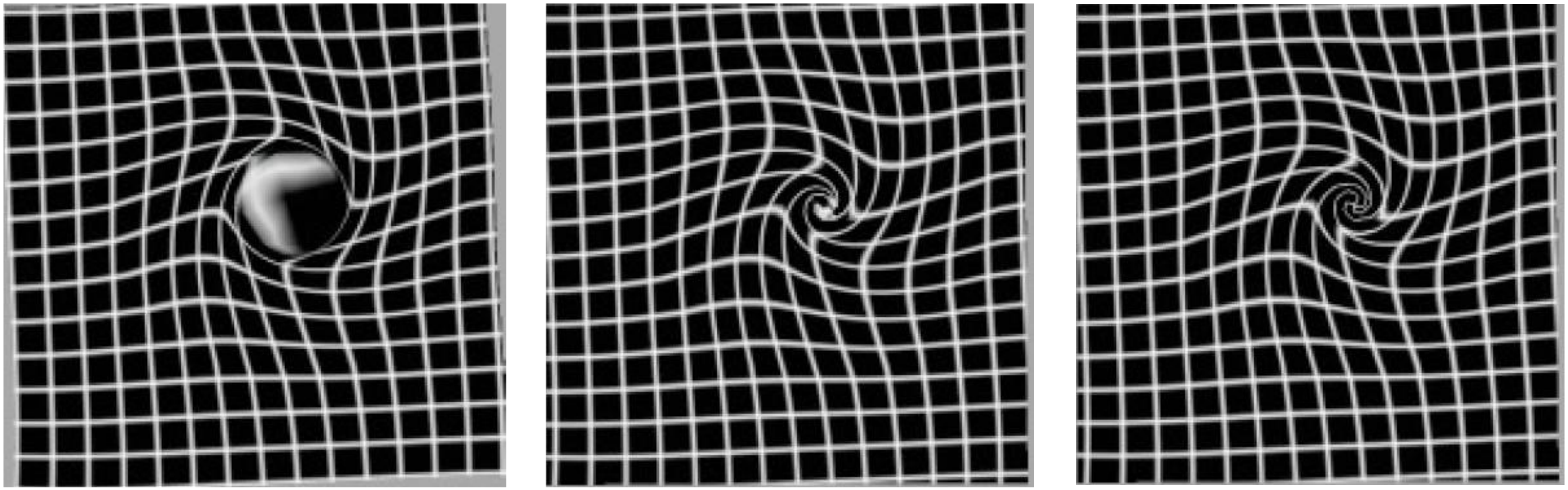

N. Max, B. Becker, Flow Visualization Using Moving Textures, Data Visualization Techniques, John Wiley & Sons, 1999

LEA

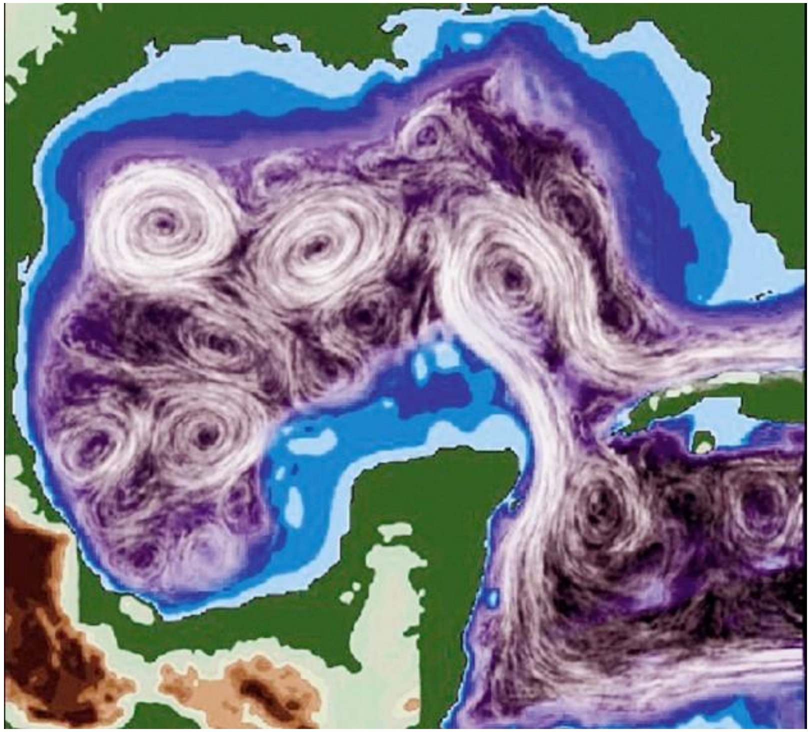 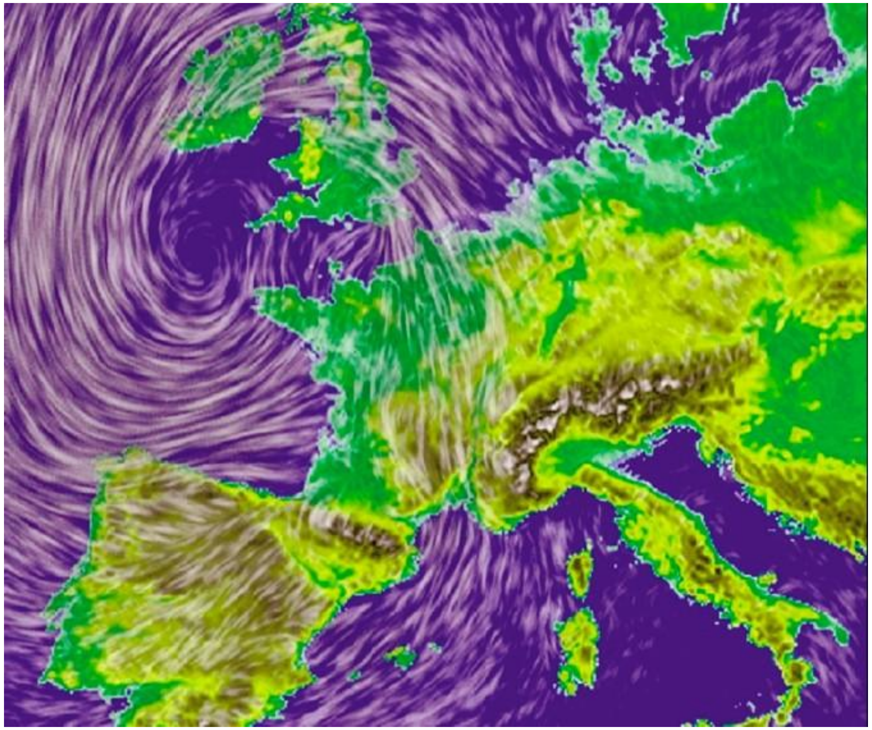

B. Jobard, G. Erlebacher, M. Y. Hussaini, Lagrangian-Eulerian Advection of Noise and Dye Textures for Unsteady Flow Visualization, IEEE TVCG 8(3), 2002

Image-Base Flow Visualization

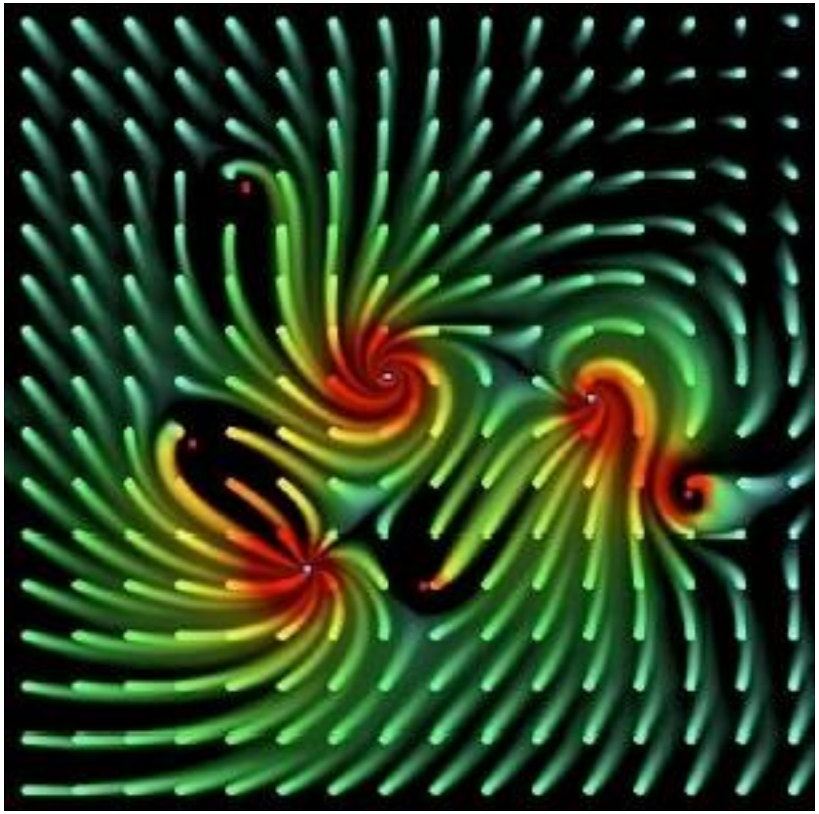

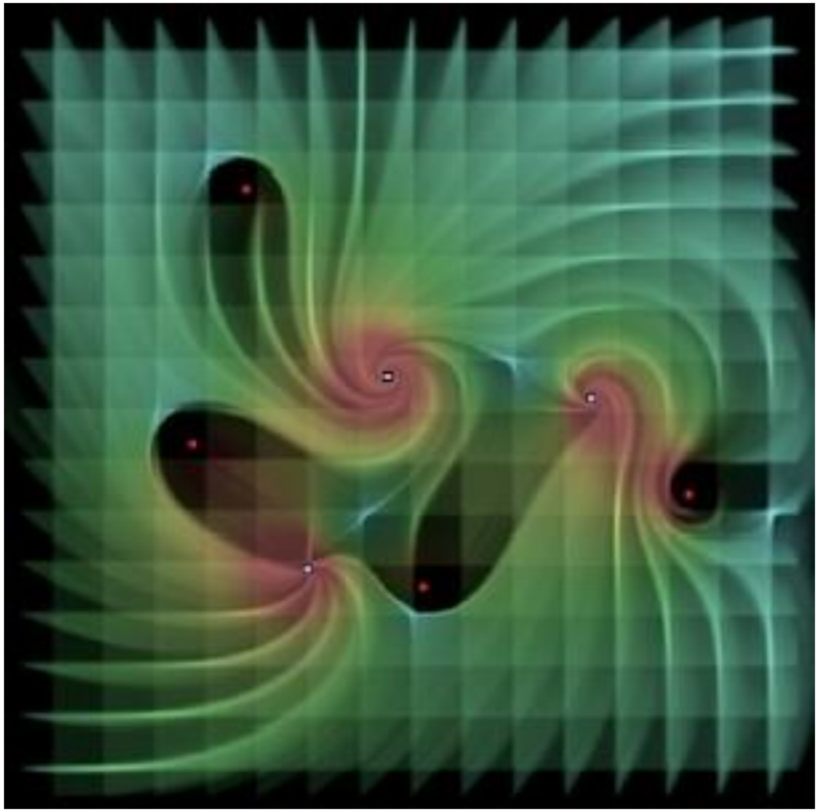

J. Van Wijk, Image Based Flow Visualization, ACM SIGGRAPH 2002

IBFV

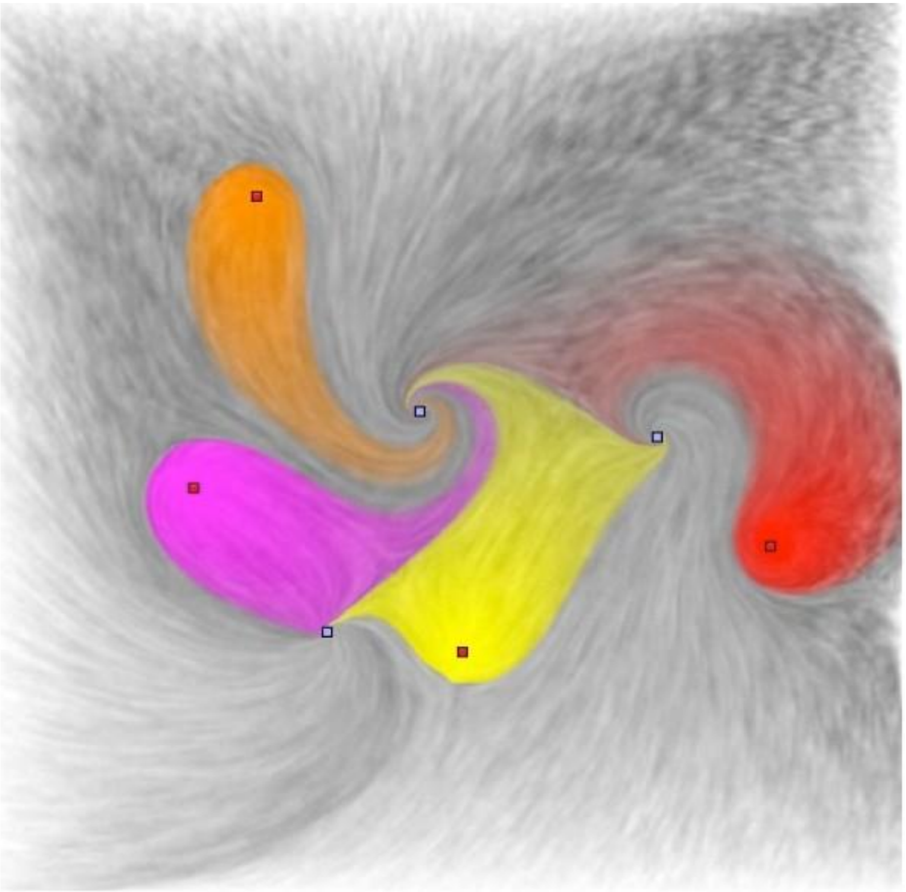

J. Van Wijk, Image Based Flow Visualization, ACM SIGGRAPH 2002

Unsteady LIC

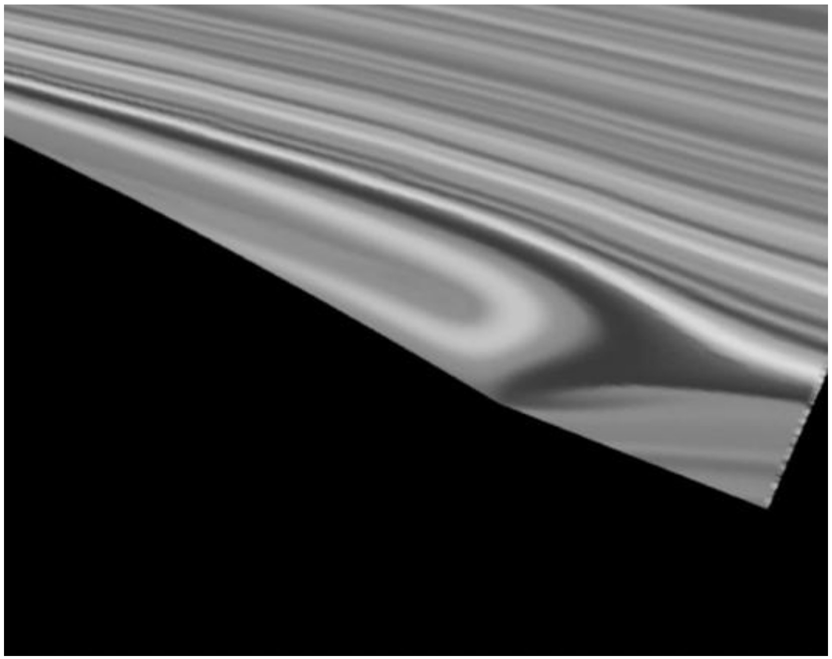

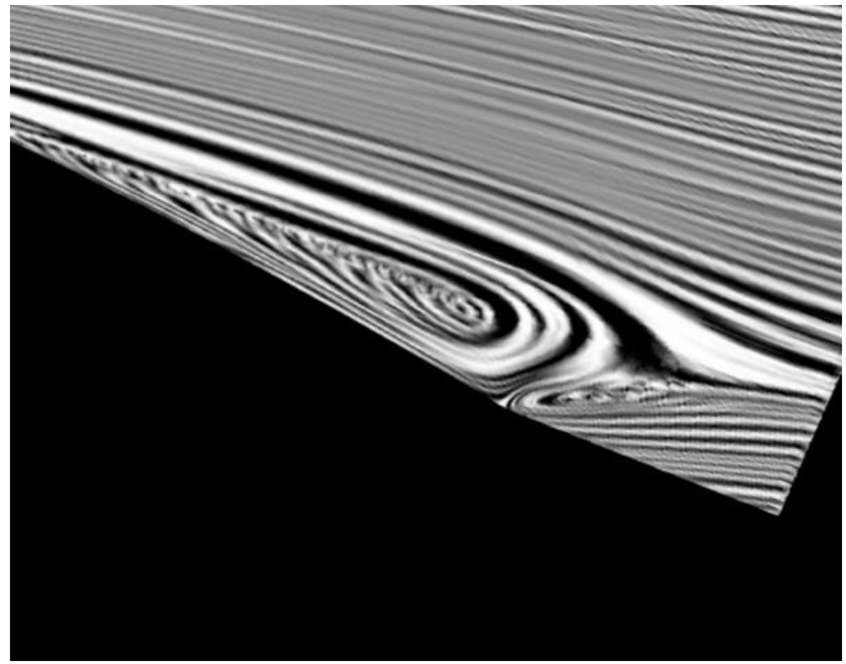

H.-W. Shen, D. Kao, A New Line Integral Convolution Algorithm for Visualizing Time-Varying Flow Fields, IEEE TVCG 4(2), 1998

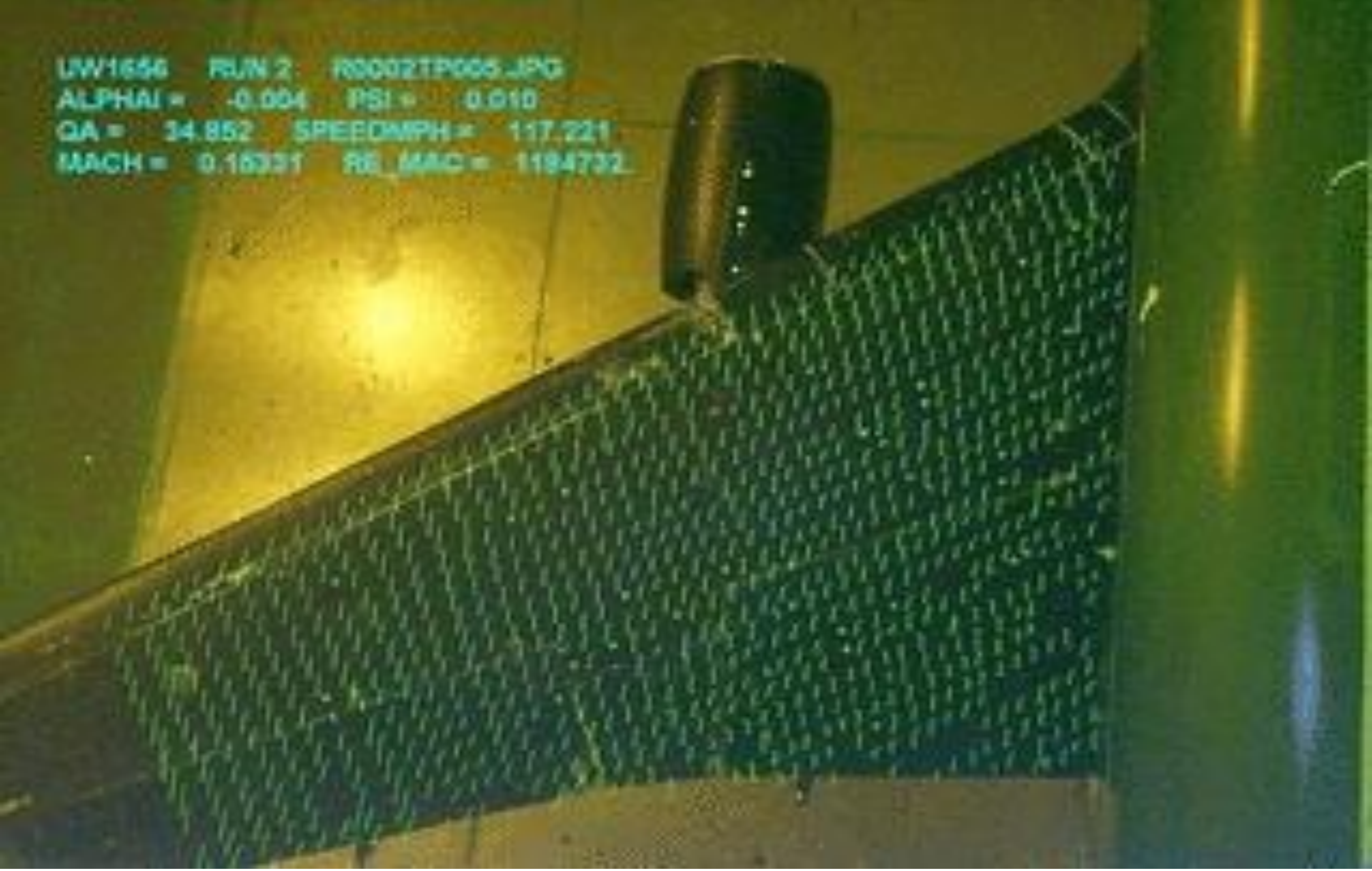

Thank You